

https://dspace.org/

Active vibration control of a structure using digital control.

Grobbelaar, Brett James

1996
https://hdl.handle.net/10539/28627

Downloaded from a DSpace repository. https://dspace.org/

Active Vibration Control of a Structure using Digital Control

Brett James Grobbelaar

A dissertation submitted to the Faculty of Engineering, University of the Witwatersrand, Johannesburg, in fulfillment of the requirements for the degree of Master of Science in Engineering.

Johannesburg, 1996

Declaration

I declare that this dissertation is my own, unaided work. It is being submitted for the Degree of Master of Science in Engineering at the University of the Witwatersrand, Johannesburg. It has not been submitted before for any degree or examination at any other University.

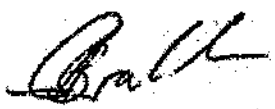

Brett James Grobbelaar

12th day of MARCH 19 96

Abstract

This dissertation covers the work done on structural vibration control research from a mechanical engineering background. A cantilevered beam is used as a test structure and an analytical model describing the beam is developed. Modal parameter estimation techniques are used to extract the modal parameters used in the analytical model. Two structural vibration control techniques are evaluated by comparing both theoretical and experimental results. Digital control methods are used to implement these control techniques, with the TMS320C30 digital signal processing card used as the digital controller. The use of a digital signal processing based system proved to be successful, however, the number of channels available were limiting. The direct velocity feedback technique is found to be a useful control tool, whilst the results pertaining to the Modified Independent Modal Space Control method are not conclusive.

Acknowledgements

I would like to acknowledge my family and Lisa for their continued support and belief in me. My brother, Grant, gets a special mention for his help and understanding.

Thank you to my supervisor Dr Brian Wigdorowitz for stepping in at the last minute.

Contents

Declaration ii

Abstract iii

Acknowledgements iv

Contents v

List of Figures viii

List of Tables x

1 Introduction 1

1.1 Historical development of control in engineering 1

1.2 Structural control 2

1.3 Problem statement and Research Objectives 2

1.4 Overview of the dissertation 3

2 Continuous system dynamics and transfer functions 4

2.1 Theoretical development of the governing equations 4

2.1.1 Continuous systems 4

2.1.2 Governing equations of beam dynamics 4

2.1.3 Theoretical transfer functions 6

2.2 Experimental extraction of modal parameters 14

2.2.1 Experimental methods 15

2.2.2 Extracting the frequency response functions 16

2.2.3 Parameter estimation 17

2.3 Synthesis of the mathematical model 19

3 Continuous Vibration control methods 21
3.1 Control systems 21
3.2 Overview of research done in structural control 22
3.2.1 Early publications relating to structural control 22
3.2.2 Research relating to smaller structures 23
3.2.3 Alternative control techniques 24
3.3 Feedback control 26
3.4 Controlling continuous vibration 27
3.4.1 State variable feedback 28
3.5 Direct velocity feedback 29
3.5.1 Accounting for modal coupling 31
3.6 MIMSC method 32

4 Application of Control to the Beam 35
4.1 Uncontrolled response of the cantilevered beam 35
4.1.1 The block diagram of the cantilevered beam 35
4.1.2 Forced response 36
4.2 Direct velocity feedback 38
4.2.1 Block diagram 38
4.2.2 Control constant determination 40
4.2.3 Controlled response 42
4.3 MIMSC method 46
4.3.1 Block diagram 46
4.3.2 Controlled response 46
4.4 Discussion 49
4.4.1 Direct velocity feedback vs. MIMSC 50

5 Experimental overview and results 52
5.1 Experimental set-up 52
5.1.1 Hardware considerations 53
5.1.2 Sensors 54
5.1.3 Actuators 54
5.1.4 Signal conditioners 55
5.1.5 Controller 55
5.2 Digital filtering 56
5.2.1 Specific filters 56

5.2.2 Integration 57
5.3 Input disturbance 60
5.4 Implementation 61
5.4.1 Uncontrolled response 61
5.4.2 Direct velocity feedback 63
5.4.3 The MIMSC method 67
5.5 Discussion 68

6 Conclusions and Recommendations **69**
6.1 Conclusions 69
6.1.1 General 69
6.1.2 Control Techniques 69
6.1.3 Digital control 70
6.2 Recommendations for further work 70

References **72**

List of Figures

2.1 Free body digram of the element of the vibrating beam 5
2.2 The system showing the beam, actuator and sensors. 6
2.3 The system to be modelled 7
2.4 The homogeneous cantilevered beam. 12
2.5 Frequency response function at position 1. 17
2.6 Frequency response function at position 2. 18

3.1 The elements of an open loop control system. 22
3.2 The elements of a closed loop control system. 22
3.3 A scalar element with and without feedback. 27
3.4 The plots of x^2 and $x^2/(x^2+1)$. 27

4.1 The block diagram showing the uncontrolled dynamics. 36
4.2 Uncontrolled response at position 1. 37
4.3 Uncontrolled response at position 2. 37
4.4 The block diagram for velocity feedback control law. 39
4.5 A plot of the absolute value of the physical displacement. 41
4.6 A plot of the absolute value of the physical displacement multiplied through by the time function y. 41
4.7 A plot of the objective function versus control constants. 43
4.8 A plot of voltage versus the control constants. 43
4.9 Controlled forced response at position 1. 44
4.10 Controlled forced response at position 2. 44
4.11 Voltage applied to the actuator. 45
4.12 Voltage applied to the actuator with attention given to the initial displacement. 45
4.13 Block diagram for the MIMSC method. 47
4.14 Controlled response at position 1, using the MIMSC method. 48
4.15 Voltage applied to the actuator for the controlled response, using the MIMSC method. 48

4.16 Controlled response at position 1, using the MIMS method with a smaller magnitude disturbance. 49
4.17 Voltage applied to the actuator for the controlled response, using the MIMSC method with a smaller magnitude disturbance. 50

5.1 Spring steel beam and dimensions 52
5.2 A typical Chebyshev type–II filter. 56
5.3 Low–pass filter containing only mode 1 frequency elements. 57
5.4 Low–pass filter containing mode 1 and 2 frequency elements. 58
5.5 High–pass filter containing mode 2 and higher frequency elements. . 58
5.6 Band–pass filter containing only mode 3 frequency elements. 59
5.7 The trapezoid between samples. 59
5.8 Frequency response of the integrator. 60
5.9 Force versus Time for a typical measured impulse force. 61
5.10 Uncontrolled response at position 1. 62
5.11 Uncontrolled response at position 2. 62
5.12 Block diagram of the direct velocity feedback system. 63
5.13 Experimental setup for the direct velocity feedback system. 63
5.14 Controlled forced response using analogue filters, at position 1. . . . 64
5.15 Controlled forced response using analogue filters, at position 2. . . . 64
5.16 Controlled forced response using digital filters, at position 1. 65
5.17 Controlled forced response using digital filters, at position 2. 65
5.18 Controlled forced response without filters, at position 1. 66
5.19 Controlled forced response without filters, at position 2. 66
5.20 Block diagram for the MIMSC control theory. 67
5.21 Controlled forced response using the MIMSC technique. 67

List of Tables

2.1 Constants for the cantilevered beam. 14
2.2 The first five natural frequencies of the beam. 14
2.3 Modal parameters predicted theoretically, for the first five modes. . . 14
2.4 Mode shape matrix at points 1 and 2. 15
2.5 Modal parameters determined, for the first five modes. 18
2.6 Mode shape matrix determined(scaled for unity modal mass). 18

5.1 Spring steel beam properties 52

Chapter 1

Introduction

1.1 Historical development of control in engineering

With the advent of electronic valve circuits and their uses, control engineering became primarily the domain of the electrical engineer. The electrical engineer had the difficult task in designing and building complex electrical circuits which required control. A large amount of research was invested into the development of electronic circuit design that could also be used to implement control laws. This has led to modern day technology and the use of digital technology. With the successful development of these electrical systems it was realised how much more could be monitored and controlled within the engineering environment.

In early applications, control was used in large processes, where it was required to keep the correct temperature, pressure or flowrate throughout the plant. An example of such a process is the boiler control required for power stations. This type of process control represents a specific area in which a substantial effort has been invested and is ongoing with regard to the control field. It is an area where factors such as rise time are represented in minutes, hours or even days (the control actions can also have economic implications involving millions of rands). For this very reason research in this particular area has been extensive, which has led to the extensive use of the digital controller. Although, the analogue system is much faster, the digital controller offers versatility and makes comparison between two different controllers a much simpler task.

With the development of high speed microprocessors the task of physically implementing complex control laws has become more promising. The need of improved computing power is an essential aspect in controlling a complex plant.

These types of plants are found in everyday mechanical systems, notably mechanical structures. Now with the need, for example, to send a structure into outer space, and the structure being made from light weight materials which showed an inherent flexibility, mechanical engineers started to employ active control methods in order that the structure was stable when being perturbed. The use of control methods allowed engineers to use improved design methods as well as light weight materials to design structures, without the risk of human injury or fatality.

It was from this type of research together with the realisation that vibration control could be successful with the use of improved electronic circuitry, that extensive

research in the field of vibration control is currently being conducted [6, 11, 25, 36, 53].

1.2 Structural control

Part of the research in active control of structures addresses the structural control of large space structures (LSS). This seems to be due to the funding avaliable, especially from NASA, for work done on structural control for structures such as solar panels, antennae and the like. The LSS like any other mechanical structure which is light in weight and flexible, usually exhibits undesirable dynamic characteristics, adversely affecting its design function. However, if vibration control of some sort could be introduced into the system, then the structure could become usable, if not ideal.

The inherent properties of structures as well as their flexibility poses a number of difficulties when designing a control system

- The first aspect to consider is the fact that a structure is a distributed parameter system. To design and practically implement a distributed control action is impossible. Hence, the control action which generates a finite number of control forces must be employed throughout the distributed structure to control the system in its entirety.
- The flexibility of these structures then initiates the problems associated with undesirable dynamic response to a disturbance. This poses a demanding task in controlling the vibration in flexible structures.

These considerations have been addressed with varying degrees of success by various researchers throughout the world, as discussed in Chapter 3.

1.3 Problem statement and Research Objectives

The discussion on the literature dealing with structural vibration control, as presented in Chapter 3, gives the misleading impression that sufficiently good solutions to the problem of vibration in structures have been found. This however, is not entirely true as becomes evident in the dissertation and continued research is necessary to improve the control methods applied in the active vibration control of flexible structures [2].

Many of the papers discussed in Chapter 3 outline the problems leading to instability of a plant for various reasons, which will become clear as the governing equations of the structure to be controlled and the control laws are presented. Therefore more research is still required to obtain stable control systems that will meet given specifications and remain stable for any input disturbance.

Another area that still needs extensive research is the use of digital controllers in an attempt to limit unwanted vibration. Few papers dealing directly with structural vibration control discuss the use of digital controllers. However, many researchers [9, 11, 15] show that the next step in further active vibration research in the same field would be the use of digital signal processors as the controllers for a controlled system.

The objective of this research is to analytically and experimentally investigate:

1. various control techniques in the active vibration control of flexible structures
2. digital implementation of the control techniques investigated.

A number of tasks must be completed to achieve these objectives, they are:

- To develop a test structure consistent with previous work; it should also be easy to manufacture and be cost effective.
- To develop a mathematical model that will accurately describe the test structure. The model should agree with experimental results for both free and forced vibration.
- Select relevant control techniques and present a theoretical background to the control method. Show analytical results pertaining to the control methods and the test structure.
- Implement a digital control system, using the control techniques selected and available hardware.
- Evaluate the control methods and compare experimental and analytical results.

In addressing the objectives that were set, the following approach was adopted:

1. two of the more prominent techniques, the direct velocity feedback and the MIMSC techniques, were applied
2. the control was digitally implemented using the TMS320C30 DSP card.

The results from the direct velocity feedback method showed an improvement on the uncontrolled dynamics, whilst the MIMSC results were inconclusive.

1.4 Overview of the dissertation

The tasks given in section 1.3 were addressed as follows:

Chapter 2 outlines the dynamics of continuous systems and the development of a theoretical transfer function of the system to be controlled. The experimental extraction of the modal parameters is discussed, and a comparison between the use of theoretical and experimental modal parameters is presented.

Chapter 3 discusses continuous vibration control methods, with an emphasis on state variable feedback. The mathematical equations for the control techniques considered in this research are developed and discussed.

Chapter 4 compares the numerical results of the direct velocity feedback and Modified Independent Modal Space Control (MIMSC) methods. The simulations are carried out using SIMULINK [50] running on MATLAB [38].

Chapter 5 presents the experimental implementation of the control methods. The results obtained from the implementation are discussed and compared to the simulated results.

The conclusions of the research together with recommendations for future work are presented in Chapter 6.1.

Chapter 2

Continuous system dynamics and transfer functions

2.1 Theoretical development of the governing equations

2.1.1 Continuous systems

An example of a continuous system is that of an Euler–Bernoulli beam. The inherent properties of a continuous system are distributed along is entire length and are properties such as mass, elasticity and damping. Although, many complex continuous systems are modelled as discrete systems, the formulation of the equations governing the continuous system gives an insight into the system and may be helpful in modelling the equivalent discrete system.

Continuous system modelling, is more complex than discrete system modelling, since the vibratory motion is described in terms of a spatial and a time dependent variable. Other factors to consider are the manner of support of the system as well as the elasticity of the structure.

The development of the governing equations of the beam are necessary for developing an understanding of the fundamental dynamics of the system, allowing a more effective control system to be designed for the particular problem.

2.1.2 Governing equations of beam dynamics

Since mass and stiffness are distributed along the length of the beam, the equations must take the form of partial differential equations. In addition certain assumptions are made that may limit the validity of the governing equations, and therefore these are outlined at the outset:

- The rotary inertia of the beam is neglected. The rotary inertia comes about from a small amount of rotation of the beam due to bending of the beam. Since lateral vibrations of the beam are being considered, the beam vibrates due to bending and some rotation must be present. However, the rotary inertia

compared to its length. The effect of rotary inertia results in an increase in effective mass and hence a lowering of the natural frequencies. This effect is more pronounced at higher frequencies and hence more influential on the higher modes.

- The shear deformation across the depth of the beam element is neglected. As discussed above the rotation is assumed to be entirely due to bending of the beam element. For slender beams the effects of shear deformation may be neglected.
- Damping is neglected. As long as the structure is lightly damped (flexible), the neglecting of the damping mechanisms will not have a significant effect on the overall system dynamic behaviour.

It is evident from the above discussion that if the system to be modelled and hence controlled is flexible and slender, the assumptions are justified. Therefore the standard approach of considering a small element of the beam and equating the moments and shear force can be employed.

Consider a free body diagram of a beam element, shown in Figure 2.1. Summing

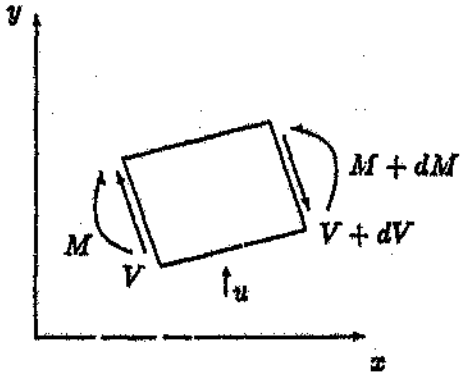

Figure 2.1: Free body digram of the element of the vibrating beam

the moments M about any point on the right hand side of the beam yields

$$\frac{\partial M}{\partial x} = V \tag{2.1}$$

where V is the shear force. From a force balance performed on the element, we obtain

$$m_l \frac{\partial^2 u}{\partial t^2} = w(x,t) + \frac{\partial V}{\partial x} \tag{2.2}$$

where u is the displacement of the element, this is compared with
y which is the direction of vibration in general coordinates
m_l is the mass per unit length and
$w(x,t)$ is the external force.

Using equation 2.1 and equation 2.2 together, we get

$$m_l \frac{\partial^2 u}{\partial t^2} = w(x,t) + \frac{\partial^2 M}{\partial x^2} \tag{2.3}$$

It may be shown, by using bending theory [51], that

$$EI\frac{\partial^2 u}{\partial x^2} = -M \tag{2.4}$$

where E is the Young's Modulus of elasticity and
I is the moment of inertia.

Substituting equation 2.4 into equation 2.3 yields

$$m_l\frac{\partial^2 u}{\partial t^2} = w(x,t) - \frac{\partial^2}{\partial x^2}\left(EI\frac{\partial^2 u}{\partial x^2}\right) \tag{2.5}$$

If m_l, E and I are constant along the length of the beam, then equation 2.5 can be rewritten as

$$\frac{\partial^2 u}{\partial t^2} + a^2\frac{\partial^4 u}{\partial x^4} = \frac{w(x,t)}{m_l} \tag{2.6}$$

where $a^2 = \frac{EI}{m_l}$.
Equation 2.6 is the governing equation of an Euler–Bernoulli beam.

2.1.3 Theoretical transfer functions

In order that a control system can be designed to limit the vibration in a vibrating beam, the governing equations are traditionally given as a set of ordinary differential equations or in terms of a number of transfer functions. This is the classical approach and will be adopted throughout this dissertation.

The system to be modelled

To represent equation 2.6 in terms of a set of ordinary differential equations (and there are infinitely many), the complete system to be controlled must be known. Therefore Figure 2.2 shows the beam to be controlled and its relevant components.

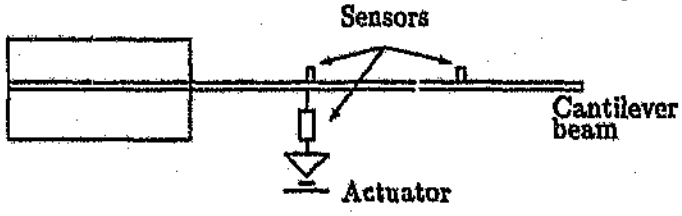

Figure 2.2: The system showing the beam, actuator and sensors.

The actuator is a loud speaker (coil winding) attached to a force transducer and to the beam. The effect that the actuator has on the beam is an increase in mass rather than stiffness since the force transducer is rather heavy. The attachment to the beam is a stinger and therefore attaches over a very small area, hence a point mass is added to the system, having the effect of lowering the natural frequencies.

Accelerometers are used as feedback sensors. However, any transducer in contact with the beam will have a mass and if the system is flexible, the mass of the transducers will alter the dynamic characteristics of the system. Therefore additional point masses are added to the beam at each point where an accelerometer exists.

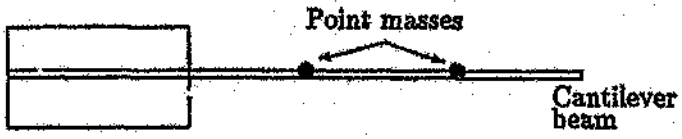

Figure 2.3: The system to be modelled

Solution of the beam equation

The technique used to determine the solution of equation 2.6 employs the separation of variables method. To explain this, a more detailed discussion of the system to be controlled is given, in terms of the generalised eigenvalue problem [39, 51]. The Laplace transformation is then used to map the equations into the s-domain and hence develop the transfer function. The generalised eigenvalue problem allows the time and space dependent variables to be separated and develops a set of equations governing the time dependent solution.

The general formulation of the eigenvalue problem states, if we have a function z of one or two independent spatial variables, the expression

$$\mathrm{L}(z) = a_0 z + a_1 \frac{\partial z}{\partial x} + a_2 \frac{\partial z}{\partial y} + a_3 \frac{\partial^2 z}{\partial x^2} + a_4 \frac{\partial^2 z}{\partial x \partial y} + \cdots \tag{2.7}$$

in which $a_0, a_1, \cdots$ are known functions of the spatial variables x and y, represents a linear homogeneous differential expression for z. The expression $\mathrm{L}(z)$ is a combination of the function z and its derivatives through order p. Therefore the linear differential operator is of the form

$$\mathrm{L} = a_0 + a_1 \frac{\partial}{\partial x} + a_2 \frac{\partial}{\partial y} + a_3 \frac{\partial^2}{\partial x^2} + a_4 \frac{\partial^2}{\partial x \partial y} + \cdots \tag{2.8}$$

For the present problem, the beam equation is represented in terms of a single spatial variable (x). Using this simplification, equation 2.8 can be written as

$$\mathrm{L} = a_0 + a_1 \frac{\partial}{\partial x} + a_2 \frac{\partial^2}{\partial x^2} + a_3 \frac{\partial^3}{\partial x^3} + \cdots \tag{2.9}$$

where $a_0, a_1, \cdots$ are known functions of x only.

Therefore equation 2.6, for a structure that is homogeneous along its length, can be expressed as

$$\mathrm{M}(\ddot{u}) + \mathrm{L}(u) = \frac{z(x,t)}{EI} \tag{2.10}$$

where $\ddot{u}$ represents the second derivative of displacement with respect to time. M and L are special cases of the generalised linear differential operators (equation 2.9) and for this particular problem are defined as

$$\mathrm{M} = \frac{m_l}{EI} \tag{2.11}$$

$$\mathrm{L} = \frac{\partial^4}{\partial x^4} \tag{2.12}$$

The model is developed in three stages:

1. The first stage is the development of the free response, without the inclusion of the point masses.
2. The second stage is the free response of the system, with the inclusion of the point masses.
3. The third stage employs the eigenfunctions found in stage 2 to solve for the forced response.

STAGE 1: Free response

For the free response, the externally acting force (on the beam) is equal to zero, therefore from equation 2.11

$$\mathbf{M}(\ddot{u}) + \mathbf{L}(u) = 0 \tag{2.13}$$

Separating the time dependent and spatial variables

$$u(x,t) = q(t)\phi(x) \tag{2.14}$$

where q is a function of t and
ϕ is a function of x.

Substituting into equation 2.13, we obtain

$$\frac{\ddot{q}}{q} = -\frac{\mathbf{L}(\phi)}{\mathbf{M}(\phi)} = -\lambda^2 \tag{2.15}$$

Therefore

$$\mathbf{L}(\phi) = \lambda^2 \mathbf{M}(\phi) \tag{2.16}$$

The function ϕ is referred to as the eigenfunction and is a function of the spatial variable x only (compare this to the eigenvector in the discrete system). λ is called the eigenvalue and represents the natural frequency of the system.

Associated with equation 2.16, are four boundary conditions that the function ϕ must satisfy along the boundary of the chosen domain Σ. The boundary conditions are of the form [39]

$$\mathbf{B}(\phi) = \lambda^2 \mathbf{C}(\phi) \tag{2.17}$$

As before $\mathbf{B}$ and $\mathbf{C}$ are linear differential operators of the form given in equation 2.9. The intent is now to solve for λ^2 for a non-diminishing eigenfunction (ϕ) so that ϕ satisfies the boundary conditions at each point along that boundary.

Consider the case where the eigenvalue does not appear in the boundary condition equations, that is

$$\mathbf{B}(\phi) = 0 \tag{2.18}$$

This occurs when no inertial load is present at the tip of the beam [51]. This is the case in this research.

From equations 2.16 and 2.18, the eigenvalue problem is said to be *self-adjoint* if for any two arbitrary functions v and w

$$\int_\Sigma v\mathbf{L}(w)d\Sigma = \int_\Sigma w\mathbf{L}(v)d\Sigma \tag{2.19}$$

and

$$\int_\Sigma v\mathbf{M}(w)d\Sigma = \int_\Sigma w\mathbf{M}(v)d\Sigma \tag{2.20}$$

$$\tag{2.21}$$

hold true. Whether a system is self-adjoint or not can be determined by means of integrating by parts (see Tse et al. [51] pp 273–275).

The orthogonality property can be extracted by considering two distinctive eigenvalues λ_r and λ_s, with ϕ_r and ϕ_s being the corresponding eigenfunctions. Since the governing equations are a self-adjoint eigenvalue problem,

$$\mathrm{L}(\phi_r) = \lambda_r^2 \mathrm{M}(\phi_r) \tag{2.22}$$

and (2.23)

$$\mathrm{L}(\phi_s) = \lambda_s^2 \mathrm{M}(\phi_s) \tag{2.24}$$

Multiplying equation 2.22 by ϕ_s and equation 2.24 by ϕ_r, subtracting the one equation from the other and integrating over the domain Σ results in

$$\int_\Sigma [\phi_s \mathrm{L}(\phi_r) - \phi_r \mathrm{L}(\phi_s)] d\Sigma = \int_\Sigma [\lambda_r^2 \phi_s \mathrm{M}(\phi_r) - \lambda_s^2 \phi_r \mathrm{M}(\phi_s)] d\Sigma \tag{2.25}$$

Since the eigenfunctions ϕ_r and ϕ_s are solutions to the self-adjoint eigenvalue problem,

$$\int_\Sigma \phi_s \mathrm{L}(\phi_r) d\Sigma = \int_\Sigma \mathrm{L}(\phi_s) d\Sigma \tag{2.26}$$

and (2.27)

$$\int_\Sigma \phi_s \mathrm{M}(\phi_r) d\Sigma = \int_\Sigma \phi_r \mathrm{M}(\phi_s) d\Sigma \tag{2.28}$$

Hence equation 2.25 reduces to

$$(\lambda_r^2 - \lambda_s^2) \int_\Sigma \phi_r \mathrm{M}(\phi_s) d\Sigma = 0 \tag{2.29}$$

But in general $\lambda_r \neq \lambda_s$, therefore

$$\int_\Sigma \phi_r \mathrm{M}(\phi_s) d\Sigma = 0 \text{ for } \lambda_r \neq \lambda_s \tag{2.30}$$

which is known as the general orthogonality condition. In addition it follows directly from equation 2.25 that

$$\int_\Sigma \phi_r \mathrm{L}(\phi_s) d\Sigma = 0 \text{ for } \lambda_r \neq \lambda_s \tag{2.31}$$

Hence for the expression $\mathrm{L}(\phi) = \lambda^2 \mathrm{M}(\phi)$ as per equation 2.24, the orthogonality condition can be expressed as

$$\int_\Sigma \phi_r \mathrm{M}(\phi_s) d\Sigma = \begin{cases} 0 & \text{for } r \neq s \\ a_r & \text{for } r = s \end{cases} \tag{2.32}$$

where Σ denotes the integration domain which is the entire solid and
a_r is called the modal mass by definition.

Note that for the special case where M is not a differential operator, but simply a function of the spatial coordinate as is the case for a cantilevered beam, the orthogonality condition becomes

$$\int_\Sigma \mathrm{M} \phi_r \phi_s d\Sigma = 0 \text{ for } \lambda_r \neq \lambda_s \tag{2.33}$$

Therefore equation 2.32 for a cantilevered beam may also be expressed as

$$\int_{\Sigma} \mathrm{M}\phi_r\phi_s d\Sigma = \begin{cases} 0 & \text{for } r \neq s \\ a_r & \text{for } r = s \end{cases} \tag{2.34}$$

STAGE 2: Extension to point masses
Since the inclusion of a number of point masses along the beam exists, equation 2.10 must be modified, yielding

$$\mathrm{P}(\ddot{u}) + \mathrm{L}(u) = 0 \tag{2.35}$$

where

$$\mathrm{P} = \frac{m_l}{EI} + \frac{\sum m_i \delta(x - x_i)}{EI} \tag{2.36}$$

where m_i is the ith point mass,
x_i is the location of the ith point mass and
δ is the generalised Dirac delta function.

Now again separating the variables, yields

$$\mathrm{L}(\phi) = \omega^2 \mathrm{P}(\phi) \tag{2.37}$$

or

$$\mathrm{L}(\phi) = \omega^2 \left[\frac{m_l \phi}{EI} + \frac{\sum m_i \delta(x - x_i)\phi}{EI}\right] \tag{2.38}$$

As before this is a representation of the generalised eigenvalue problem. For this particular case, ω is the eigenvalue and ϕ is the eigenfunction. It is clear that the inclusion of the point masses has changed the values of the natural frequencies (intuitively it should lower the natural frequencies).

Choosing a particular eigenfunction,

$$\mathrm{L}(\phi_r) = \omega_r^2 \left[\frac{m_l \phi_r}{EI} + \frac{\sum m_i \delta(x - x_i)\phi_r}{EI}\right] \tag{2.39}$$

Using equation 2.16, and substituting equation 2.39 for $\mathrm{L}(\phi_r)$ gives

$$\lambda^2 \mathrm{M}(\phi_r) = \omega_r^2 \left[\frac{m_l \phi_r}{EI} + \frac{\sum m_i \delta(x - x_i)\phi_r}{EI}\right] \tag{2.40}$$

Multiplying equation 2.40 through by a different eigenfunction, say ϕ_n and integrating over the entire solid

$$\int_{\Sigma} \lambda^2 \phi_n \mathrm{M}(\phi_r) d\Sigma = \int_{\Sigma} \omega_r^2 \left[\phi_n \mathrm{M}(\phi_r) + \frac{\sum m_i \delta(x - x_i)\phi_r \phi_n}{EI}\right] d\Sigma \tag{2.41}$$

Now referring to equation 2.34 and observing the orthogonality of the eigenfunction, we reduce equation 2.41 to

$$\lambda_r^2 a_r = \omega_r^2 \left[a_r + \sum \frac{m_i \phi_r^2(x_i)}{E(x_i)I(x_i)}\right] \tag{2.42}$$

Therefore

$$\omega_r^2 = \frac{\lambda_r^2}{1 + \frac{1}{a_r} \sum \frac{m_i \phi_r^2(x_i)}{E(x_i)I(x_i)}} \tag{2.43}$$

The intuition that by including the point masses the natural frequencies would be lowered is clearly shown in equation 2.43.Note that the natural frequency before the inclusion of the point masses was λ and now it is given by ω.

STAGE 3: Forced response
The solution for the forced response is carried out in the same way as for the free response. Eigenfunctions from the first stage are used to construct a basis, which forms the solution of the forced response. Therefore as before

$$u_r(x,t) = \sum_r q_r(t)\phi_r(x) \tag{2.44}$$

Now, rewriting equation 2.6, but including the point masses and using the fact that $u_r(x,t) = \sum_r q_r(t)\phi_r(t)$

$$\ddot{q}_r\left[\frac{m_l\phi_r}{EI} + \frac{\sum m_i\delta(x-x_i)\phi_r}{EI}\right] + q_r\mathrm{L}(\phi_r) = \frac{w(x,t)}{EI} \tag{2.45}$$

Using the relation $\mathrm{L}(\phi_r) = \lambda_r^2\mathrm{M}(\phi_r)$,

$$\ddot{q}_r\left[\frac{m_l\phi_r}{EI} + \frac{\sum m_i\delta(x-x_i)\phi_r}{EI}\right] + q_r\lambda_r^2\mathrm{M}(\phi_r) = \frac{w(x,t)}{EI} \tag{2.46}$$

Then multiplying equation 2.46 through by ϕ_n and integrating over the spatial domain,

$$\int_\Sigma \ddot{q}_r\left[\phi_n\mathrm{M}(\phi_r) + \frac{\sum m_i\delta(x-x_i)\phi_r\phi_n}{EI}\right]d\Sigma + \int_\Sigma q_r\lambda_r^2\phi_n\mathrm{M}(\phi_r)d\Sigma = \int_\Sigma \frac{w(x,t)\phi_n}{EI}d\Sigma \tag{2.47}$$

Evaluating the integrals, gives

$$\ddot{q}_r + \frac{\lambda_r^2}{1+\frac{1}{a_r}\sum\frac{m_i\phi_r^2(x_i)}{E(x_i)I(x_i)}}q_r = \frac{\int_\Sigma\frac{w(x,t)\phi_n}{EI}d\Sigma}{a_r+\sum\frac{m_i\phi_r^2(x_i)}{E(x_i)I(x_i)}} \tag{2.48}$$

Equation 2.48 can be written in the form

$$\ddot{q}_r + \omega_r^2 q_r = f_r(t) \tag{2.49}$$

where q is called the generalised or modal coordinate and
ω_r is the natural frequency of the rth mode.

This equation is of the standard second order form, without the inclusion of the damping term.

The theoretical transfer function

With the use of the loud speaker coil as an actuator, a point force is applied to the beam when a voltage is given to the speaker. The amplifier employed uses a current feedback module, allowing for a force proportional to the voltage supplied. This is noted here so that the theoretical transfer function is developed taking into account this factor.

Hence, the external force can be written as

$$w(x,t) = f_c(t)\delta(x-x_j) \tag{2.50}$$

where f_c is the force of the speaker coil, applied to the beam and
x_j is the x-coordinate at which the force acts.

Accounting for equation 2.48, leads to

$$f_r(t) = \frac{\int_\Sigma \frac{f_c(t)\delta(x-x_j)\phi_n}{EI} d\Sigma}{a_r + \sum \frac{m_i \phi_r^2(x_i)}{E(x_i)I(x_i)}} \tag{2.51}$$

Upon integrating equation 2.51 becomes

$$f_r(t) = \frac{f_c(t)\frac{\phi(x_j)}{E(x_j)I(x_j)}}{a_r + \sum \frac{m_i \phi_r^2(x_i)}{E(x_i)I(x_i)}} \tag{2.52}$$

Which can be simplified into the form

$$f_r(t) = k f_c(t) \tag{2.53}$$

Hence

$$\ddot{q}_r + \omega_r^2 q_r = k f_c(t) \tag{2.54}$$

Transforming equation 2.54 into the Laplace domain and writing it in the form of a transfer function, we obtain the relationship between the modal displacement and the force applied.

$$\frac{Q_r(s)}{F_c(s)} = \frac{k}{s^2 + \omega_r^2} \tag{2.55}$$

where $Q(s)$ is the Laplace transform of the modal displacement and
$F(s)$ is the Laplace transform of the force applied to the beam.

Solution to the theoretical transfer function

A program was written in MATLAB to develop the theoretical transfer function and find a numerical solution for the specified problem as described above. By including the action of the accelerometers and the force transducer on the beam the natural frequencies and the constant (for each mode) k of the system was calculated. Point 1 is 177mm from the base of the beam and point 2 is 300mm from the base of the beam.

In order that the theoretical solution be obtained for the above transfer function, it is first necessary to determine the natural frequencies of the beam without any point masses. Consider the homogeneous cantilevered beam with lateral vibration given in Figure 2.4

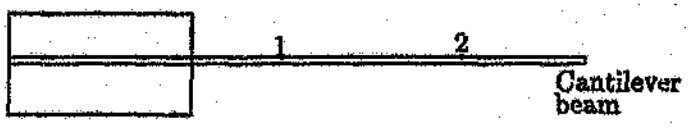

Figure 2.4: The homogeneous cantilevered beam.

As before, the beam equation for the free response is given by

$$\frac{\partial^2 u}{\partial t^2} + a^2 \frac{\partial^4 u}{\partial x^4} = 0 \tag{2.56}$$

Recalling that

$$u(x,t) = \phi(x)q(t) \tag{2.57}$$

Now substituting equation 2.57 into equation 2.56, we obtain

$$-a^2\frac{1}{\phi}\frac{d^4\phi}{dx^4} = \frac{1}{q}\frac{d^2q}{dt^2} \tag{2.58}$$

Letting each side of equation 2.58 equal ω^2

$$\frac{d^4\phi}{dx^4} + \beta^4\phi = 0 \tag{2.59}$$

$$\frac{d^2q}{dt^2} - \omega^2 q = 0 \tag{2.60}$$

where $\beta^4 = \omega^2/a^2 = m_l\omega^2/EI$.

It can be shown that the generalised solutions of equations 2.59 and 2.60 are of the form [51]

$$\phi(x) = A\sin\beta x + B\cos\beta x + C\sinh\beta x + D\cosh\beta x \tag{2.61}$$

$$q(t) = E\sin\omega t + F\cos\omega t \tag{2.62}$$

The boundary conditions for the cantilevered beam are given by

(i) $u(0,t) = 0$ and

(ii) $\frac{\partial u}{\partial x}(0,t) = 0$ for the fixed end.

(iii) $\frac{\partial^2 u}{\partial x^2}(l,t) = 0$ and

(iv) $\frac{\partial^3 u}{\partial x^3}(l,t) = 0$ for the free end.

Condition (i) yields $B + D = 0$ and condition (ii) yields $A + C = 0$. Using these results in equation 2 61, we obtain

$$\phi(x) = A(\sin\beta x - \sinh\beta x) + B(\cos\beta x - \cosh\beta x) \tag{2.63}$$

Using condition (iii)

$$0 = A(-\sin\beta l - \sinh\beta l) + B(-\cos\beta x - \cosh\beta l) \tag{2.64}$$

and from condition (iv)

$$0 = A(-\cos\beta l - \cosh\beta l) + B(\sin\beta x - \sinh\beta l) \tag{2.65}$$

leads to simultaneous equations which for a nontrivial solution for A and B, requires

$$\begin{vmatrix} -\sin\beta l - \sinh\beta l & -\cos\beta l - \cosh\beta l \\ -\cos\beta l - \cosh\beta l & \sin\beta l - \sinh\beta l \end{vmatrix} = 0 \tag{2.66}$$

Expanding equation 2.66, yields the characteristic equation

$$\cos\beta l\cosh\beta l = -1 \tag{2.67}$$

Length (mm)	Width (mm)	Thickness (mm)	Density (kg/m^3)	Young's Modulus (GPa)
400	31.5	1.6	7800	207

Table 2.1: Constants for the cantilevered beam.

Mode	Natural frequency (Hz)
1	8.32
2	52.15
3	146.03
4	286.15
5	473.03

Table 2.2: The first five natural frequencies of the beam.

Solving equation 2.67 numerically, using the constants of the beam given in Table 2.1, the values for the beam natural frequencies are obtained. The beam natural frequencies are given in Table 2.2.

These values are then inserted into equation 2.63 to obtain the natural modes. Using $\phi(x)$, together with the solution to the eigenvalue problem gives a complete theoretical solution in terms of a transfer function.

Table 2.3 gives the modal parameters as determined theoretically, while Table 2.4 contains the mode shape matrix for the first five modes, at points 1 and 2. k_{11} and

Mode	ω (Hz)	k_{11}	k_{12}
1	8.04	2.225	5.386
2	50.40	7.640	1.721
3	141.13	3.940	-6.332
4	276.57	-5.676	6.092
5	457.17	-5.991	-1.400

Table 2.3: Modal parameters predicted theoretically, for the first five modes.

k_{12} are arbitrary constants, consistent with the properties of the beam.

2.2 Experimental extraction of modal parameters

An alternative method used to develop the transfer functions governing the flexible beam is to use modal testing and extract the modal parameters experimentally. This technique incorporates the dynamics of the filters, amplifiers or actuators into the dynamics of the plant (as a single entity). Hence, the transfer function developed using this method introduces the physical properties of the system through direct measurement.

ϕ	1	0.753	1.382	0.739	-1.063	-1.121
	2	1.823	0.311	-1.188	1.141	-0.262

Table 2.4: Mode shape matrix at points 1 and 2.

2.2.1 Experimental methods

The measurement and subsequent analysis of modal parameters of a structure is known as Modal testing. Modal testing is used to determine the response of a structure to a disturbance, by measuring the following quantities

- Natural frequency (ω)
  The basic definition of a natural frequency derives from the undamped system's eigenvalues, which yield the frequencies at which free vibration of the system can take place. For damped systems, the situation becomes more complex and two alternative natural frequency parameters may be defined. The first definition derives form the oscillatory part of the free vibrating characteristic, which, being complex contains an exponential decay in addition to the free vibrating frequency. The second definition comes from the general expression of the frequency response function, and is not shown here (see [21]). The greatest amplitudes that are detected on a frequency plot of a structure for an input disturbance, will exist as a function of the system natural frequencies, and is given by $\sqrt{1-2\zeta^2}\omega_n$, where ζ is the damping ratio. These are the system eigenvalues. The natural frequency can be either damped or undamped, but for lightly damped systems the difference is negligible. Undamped natural frequency is normally expressed in radians/s (or Hz), where $\omega = 2\pi f$. Damped natural frequency, also expressed in radians/s, is given as $\omega_d = \omega_n\sqrt{1-\zeta^2}$ (where ζ is the damping ratio and is discussed further in the next point).

- Damping ratio (ζ)
  In flexible structures this value is very small (typically 0.5% of the critical value), which presents difficulties in the control system design. The damping ratio is usually expressed as a % of critical damping.

- Residue, denoted by A_{ij}^r. The residue is expressed as reference DOF i, response DOF j and mode r. The residue is a scaled quantity and can be interpreted from the frequency response function (FRF) model

$$H_{ij}(j\omega) = \sum_{r=1}^{N}\left[\frac{A_{ij}^r}{j\omega-(s-j\omega_{d_r})} + \frac{A_{ij}^{r*}}{j\omega-(s-j\omega_{d_r}^*)}\right]$$

  where H_{ij} is for example the displacement over force FRF, * denotes the complex conjugate and ω_{d_r} is the damped natural frequency of the rth mode.

- Mode shape coefficient, denoted as ψ_i^r, or ϕ_i^r for a mass normalised mode shape. The mass normalised mode shape coefficient is related to the more generalised form by

$$\phi_i^r = \frac{1}{\sqrt{a_r}}\psi_i^r$$

where a_r is the modal mass of the rth mode. The mode shape coefficients are expressed as a response DOF i and a mode r. These coefficients are assembled for all DOF's i to form the modal shape matrix. For the computer package used to curve fit the frequency response functions, the relationship between the residue and mode shape can be expressed as

$$A_{ij}^{r} = \frac{\psi_i^r \psi_j^r}{2j\omega_{d_r} a_r}$$

where j is the complex number equal to $\sqrt{-1}$. The residues are usually expressed as scaled quantities, and usually done so that a modal mass for all modes equals one ($a_r = 1$).

Modal testing methods are used because it is often difficult to measure the dynamic forces causing vibration in a structure directly. Therefore the response of the system is measured and equivalent forces are inferred. This allows an analysis of complex forced inputs without an indepth knowledge of the actual forces involved.

2.2.2 Extracting the frequency response functions

It is clear from section 2.1.3 that a transfer function exists between the actuator and each of the observation points on the beam. The transfer function is also known to be of the form

$$H_{ij}(s) = \sum_{r=1}^{N} \left[\frac{A_{ij}^{r}}{s - (s - sr)} + \frac{A_{ij}^{r*}}{s - (s - sr^*)} \right] \tag{2.68}$$

Furthermore the relationship between the output at $x = x_i$ and the input is given by

$$u(x_i, s) = H_{ij}(j\omega) V(s) \tag{2.69}$$

where $u(x_i, s)$ is the Laplace transform of the i observation point
$H_{ij}(s)$ is the transfer function
$V(s)$ is the Laplace transform of the input voltage.

The transfer function $H_{ij}(s)$ can then be experimentally extracted by dividing the signal of the structure displacement by the input voltage, which is varied over a specified frequency range. The input voltage is most commonly a sinusoid, although random excitation techniques may also be applied. The random excitation is generally for broad band excitation and reduction of cost.

The frequency response plots were extracted experimentally using a data acquisition system that is specifically designed for modal analysis, together with the accompanying software. The transfer function between the accelerometers and the force of the actuator was determined. The force transducer output was proportional to the voltage input of the actuator, since a current feedback system was used on the actuator amplifier.

A microprocessor based acquisition system specifically designed to perform modal analysis was avaliable (GenRad data acquisition system [23]). Consequently, the acquisition system has the facility to sample response data from a structure and perform real time analysis on the data so as to produce meaningful results. The

software package used [23], supplies an output voltage for the input to the actuator, and in this particular case a swept sine type voltage input was used. Four input channels on the acquisition system allowed for four simultaneous signals to be read in. Hence, the transfer function was determined by comparing the output voltage to the transducer response.

The calibration constants of the accelerometers and force transducer are taken into account by entering the values, hence the transfer function determined shows a relation between acceleration and force, not voltage from the accelerometers and voltage output from the force transducer.

At this stage all the power amplifiers are included in the loop so that when the control system is designed and implemented, all the system dynamics are taken into account. The levels of the amplifiers are kept constant throughout the sampling and testing of the beam response.

The transfer functions for two positions on the beam were measured. Only two points were used due to the fact that the digital controller only has two inputs, and consequently the analysis of one of the control laws is restricted to only the first two modes. These frequency response plots are shown in Figures 2.5 and 2.6. Figure 2.5 contains the plot of the point impedance. Figure 2.5 shows the FRF at a position

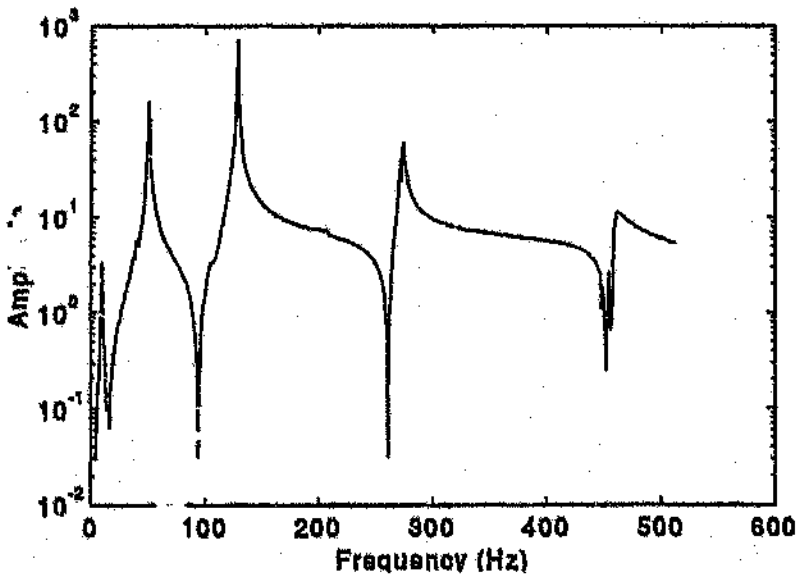

Figure 2.5: Frequency response function at position 1.

of 177mm from the base of the beam and Figure 2.6 shows the FRF at a position of 300mm form the base of the beam.

2.2.3 Parameter estimation

Once the frequency response functions had been determined, the mathematical transfer function could be calculated. The ascii data from the data acquisition system, containing information about the FRFs, was transferred to the PC where

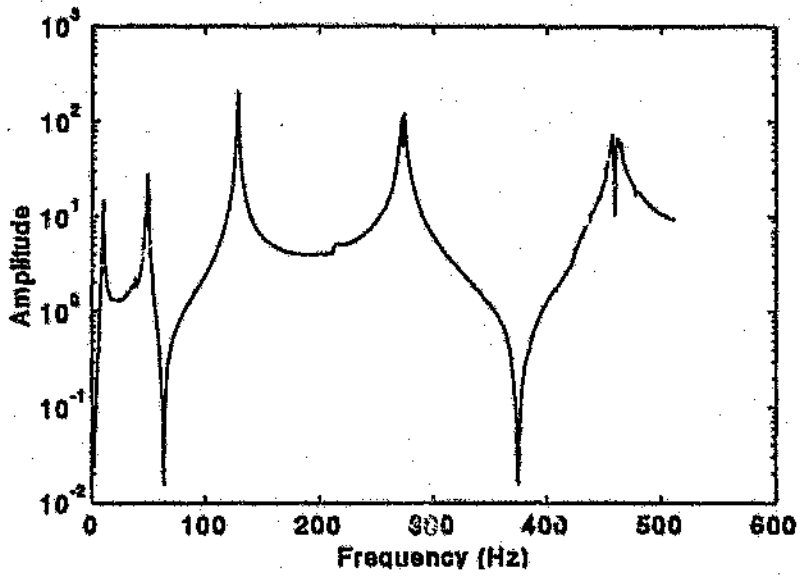

Figure 2.6: Frequency response function at position 2.

the software package to curve fit the transfer function data resides. A complex exponential parameter estimation technique [21] was employed to calculate the modal parameters. In addition, the transfer function relating displacement to force was required, and therefore the signal was integrated twice in the frequency domain, before the parameters were extracted. The mode shapes were scaled so that an equivalent modal mass of one was estimated. The parameters determined are given in Tables 2.5 and 2.6.

Mode	ω (Hz)	ζ (%)	A_{11} (s/kg) $\times 10^{-3}$	A_{12} (s/kg) $\times 10^{-1}$
1	8.72	0.74	1.911	8.525
2	48.74	0.46	4.448	-0.811
3	127.73	0.08	2.018	-0.746
4	272.24	0.31	0.195	0.430
5	458.05	0.51	0.043	0.241

Table 2.5: Modal parameters determined, for the first five modes.

ϕ	1	0.458	1.650	1.799	0.817	0.499
	2	2.041	-0.301	-0.665	1.800	2.774

Table 2.6: Mode shape matrix determined(scaled for unity modal mass).

By comparing Tables 2.3 and 2.5, the difference between the theoretical and experimentally predicted natural frequencies are small. However, the discrepancies can be attributed to the boundary conditions and the assumption of a point mass in

the place of the accelerometers and force transducer. The experimentally extracted frequency response plots, together with the complex exponential curve fitting procedure shows a better description of the action of the transducers on the beam, as well as the affect of the amplifiers on the overall system dynamics. For these reasons, the experimentally extracted modal parameters are used rather than the purely theoretical constants.

2.3 Synthesis of the mathematical model

Once the modal parameters have been found, the mathematical model can be reconstructed. Recalling that the transfer function is of the form

$$H_{ij}(s) = \sum_r \frac{A_{ij}^r}{s^2 + 2\zeta_r\omega_r + \omega_r^2} \tag{2.70}$$

Furthermore it has been shown theoretically that

$$u(x_i, t) = \sum_r q_r(t)\phi_j^r \tag{2.71}$$

and transforming this equation and using $U(x_i, s) = H_{ij}(s)F(s)$ (where $F(s)$ is the Laplace transform of the forcing function), we obtain

$$Q_r(s)\phi_j^r = \sum_r \frac{A_{ij}^r F(s)}{s^2 + 2\zeta_r\omega_r + \omega_r^2} \tag{2.72}$$

Where $Q_r(s)$ is the Laplace transform of the modal displacement q. Now choosing mode r we obtain

$$Q_r(s)\phi_j^r = \frac{A_{ij}^r F(s)}{s^2 + 2\zeta_r\omega_r + \omega_r^2} \tag{2.73}$$

Therefore

$$Q_r(s) = \frac{\frac{A_{ij}^r}{\phi_j^r}F(s)}{s^2 + 2\zeta_r\omega_r + \omega_r^2} \tag{2.74}$$

But, from section 2.2.1

$$A_{ij}^r = \frac{\phi_i^r \phi_j^r}{2j\omega_{dr}a_r} \tag{2.75}$$

Note the use of ϕ instead of ψ, since the equivalent modal mass is one ($a_r = 1$), and hence the mass normalised mode shape is equal to the more generalised form.

Combining equations 2.74 and 2.75 and noting that the mode shape is scaled for unity modal mass, we obtain

$$Q_r(s) = \frac{\frac{\phi_i^r}{2\omega_{dr}}F(s)}{s^2 + 2\zeta_r\omega_r + \omega_r^2} \tag{2.76}$$

The resulting mathematical model is of the form

$$\ddot{q}_1 + 2\zeta_1\omega_1\dot{q}_1 + \omega_1^2 q_1 = \frac{\phi_i^1}{2\omega_{d1}}f(t) \tag{2.77}$$

$$\ddot{q}_2 + 2\zeta_2\omega_2\dot{q}_2 + \omega_2^2 q_2 = \frac{\phi_i^2}{2\omega_{d2}}f(t) \tag{2.78}$$

$$\vdots$$

$$\ddot{q}_r + 2\zeta_r\omega_r\dot{q}_r + \omega_r^r q_r = \frac{\phi_i^r}{2\omega_{dr}}f(t) \tag{2.79}$$

where f is the physical force applied to the structure.

Finally, the equation determining the physical displacement at the two positions along the beam (u_1 and u_2) is given by

$$\begin{Bmatrix} u_1 \\ u_2 \end{Bmatrix} = \begin{bmatrix} \phi_1^1 & \phi_1^2 & \cdots & \phi_1^r \\ \phi_2^1 & \phi_2^2 & \cdots & \phi_2^r \end{bmatrix} \begin{Bmatrix} q_1 \\ q_2 \\ \vdots \\ q_r \end{Bmatrix} \tag{2.80}$$

Chapter 3

Continuous Vibration control methods

3.1 Control systems

There are three elements to a control system. These elements are an objective, an outcome and a link between the objective and the physical outcome. The link between the objective and outcome may be a a single device or a number of devices depending on the complexity of the problem.

It is easily visualised that in everyday life we come across a number of control systems. The refrigerator is a simple example. The objective in this case is to keep the interior of the refrigerator within a certain temperature range, which is acted on by the adjustment of the control knob. The outcome is the actual temperature range achieved, with the link (or medium) being the parts that make up the refrigerator. For this example it can be seen that many larger control systems are actually made up of a number of smaller control systems. The car is a good example of this. The car is a large control system where the objective is to travel from one point to another. This is achieved by the interaction of a number of smaller control systems, namely the brakes, the cooling system etc.

The examples given are examples of feedback control systems, which is by far the most commonly used control technique. Feedback is the use of a system outcome which is compared with the requirement (or objective) of the system and then fed back into the system to more accurately obtain the required objective. It is evident that feedback only becomes necessary when there is uncertainty in the system. This is shown by the fact that if the outcome of a system is not exactly as expected then some uncertainty must be present. It can also be seen that a feedback control system still has the three basic elements of a control system but another two elements are necessary. These are a sensing element which measures the outcome and a controller which processes the outcome and uses it to modify the input of the system.

The two control systems discussed are known as open loop and closed loop control systems. These systems are shown diagrammatically in Figures 3.1 and 3.2.

The uncertainty in a feedback system can arise from two different areas. The first is the uncertainty about the system to be controlled and the second the uncertainty derived from an external disturbance (usually caused due to the specific environment).

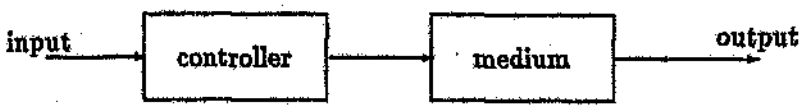

Figure 3.1: The elements of an open loop control system.

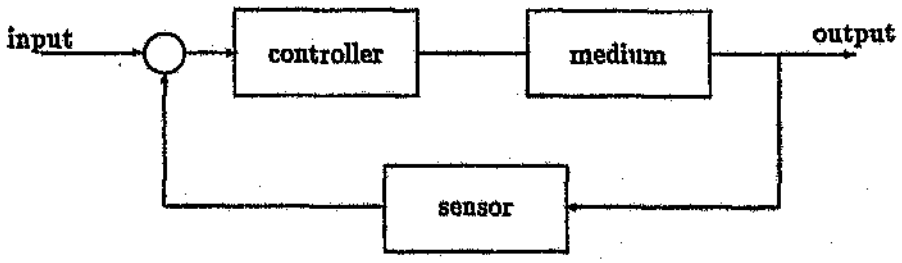

Figure 3.2: The elements of a closed loop control system.

3.2 Overview of research done in structural control

The concept of structural control has been considered since the early seventies. Today extensive research has been carried out on the various aspects relating to active vibration control in structures. This section outlines the development in this research field from the work in the early eighties when some papers of an overview nature on the subject of active vibration control were published [2].

3.2.1 Early publications relating to structural control

By 1977 it was evident some engineering researchers were discussing the need for structural vibration control, especially in LSS. Research had been done on the mathematical frameworks that would lead to full mathematical presentation of the controllers for mechanical structures. In addition many engineers were carrying out independent work that would contribute to the field of structural control as we know it today.

A summary paper by Balas [2] summarised the status of active vibration control of flexible structures up until 1982. This paper cites a large number of papers, dealing with various issues in the mechanical structures field (both applied and mathematically based). The survey discusses what solutions had been proposed up until then in order that the vibration in distributed parameter systems may be controlled. The mathematical framework dealing with the linear quadratic regulator theory, as well as its relevance to the reduced order model problem is presented. As will become clear later, when dealing with LSS, only a finite number of modes may be controlled which is only achievable with a reduced order model. By the same token, the higher order modes must be accounted for, otherwise an unstable control system results. The paper also touches on digital implementation of LSS controllers as well as adaptive control and filtering. Balas further expresses his hope that structural vibration control will be as successful as early promises had shown.

A number of papers have been published addressing various issues in the modelling and control of flexible structures.

Balas published an engineering note [4] discussing the state variable technique of direct velocity feedback. This paper showed the mathematical basis needed to implement this control method. This particular control method is still being extensively researched, and is discussed further throughout this dissertation.

Hughes [32] primarily considers the large space structure type mechanical structure. Hughes also discusses that up until then most structural analysis techniques focussed on structural–dynamical models that neglected linear–viscous damping. He stated that a model incorporating the damping matrix term shows an improved description of the overall system. Furthermore, this paper suggests a method to determine the values of the damping terms, so that the mathematical model will closely represent the real system. Therefore, by incorporating this term in the model and simply adding passive damping to the physical system, an improved response to vibration is found.

Another paper dealing with feedback control of flexible systems [3], discusses the development of the reduced order model of the plant. This model is then used in order that a stable control system be developed. The affect of the higher order modes (if they are not accounted for) is also discussed.

Joshi [34] proposes a controller for LSS, in the form of an active damper. This is essentially the direct velocity feedback technique, however, Joshi suggests that there is an optimal selection of certain parameters, to which the active damping should be applied. The paper also discusses the problems associated with control spillover (refer Chapter 2) and the controller is designed with this in mind. For the model of the system a reduced order model is used, noting that in general the maximum vibration is derived from the first few modes, which is within the bandwidth of the controller.

Hughes and Skelton [33] present a paper discussing the observability and the controllability of the flexible system, which in this particular case is a spacecraft. This paper also deals extensively with the actuator and sensor placement and selection for the particular structure.

Following further surveys [2, 24, 49] dealing with the future of structural control of large space structures, and tying the work done up until the early eighties, extensive research was published on specific topics. Hence, research in the field of structural control has developed very quickly, over the period from 1985 to present.

3.2.2 Research relating to smaller structures

More recently, smaller structures have been used to test structural vibration control theories. These smaller structures have then been compared to the large space structures.

It is important to realise the similarities in controlling large space structures as opposed to smaller structures. The control techniques are essentially the same, however, the practical implementation may be a far more demanding task when dealing with large space structures.

It has come evident that a suitable structure for use in the laboratory and comparison with large structures is the Euler-Bernoulli beam [49, 8, 7]. The most compelling reasons being the simplicity of the structure and the flexibility which comes

from the traditional Euler-Bernoulli having a large ratio of beam length to beam thickness. Due to the dimensions of the Euler-Bernoulli beam, the beam show enormous flexibility which can be directly related to the behaviour of the LSS. Hence, a large number of researchers have experimentally verified their work on either simply supported beams or the fixed–free Euler-Bernoulli beam.

Schäfer and Holzach [49] published a paper that described work that had been done on a hardware experiment used to study the active vibration control of a clamped–free flexible beam. The modal control technique implemented was based on the direct velocity feedback control. In their experiment, a flexible beam was hung vertically and clamped at one end. An electro–optical displacement sensor was used to detect motion of the beam and the displacement was acted upon by electrodynamic force actuators.

Similar work was carried out by Schaechter [48]. An experiment employing a pinned–free flexible beam was constructed, however, this flexible beam was large enough to simulate a LSS more closely. The hardware was constructed to demonstrate active shape control, active dynamic control, adaptive control and various other control approaches.

Most control techniques since 1990 are tested on flexible beams, giving a suitable standard with which to compare results. So, with the test structure in place, further research has followed two paths; the first of which concerns different control algorithms, with increasing mathematical complexity. The other concerns more of a hardware approach, optimising sensor placement and sensor and actuator selection.

3.2.3 Alternative control techniques

The most widely used and understood control technique for structural control is the direct velocity feedback technique [4, 35]. The simplicity and ease of practical implementation makes this method rather attractive as the results produced often meet the specifications of the plant. Numerous papers have been published relating to this topic, with one of the first being the paper by Balas [4]. Joshi [35] also published work on active vibration control using direct velocity feedback. He referred to this method as an energy dissipation technique and showed that a robust controller could exists despite the use of a truncated model.

The use of direct velocity feedback is a special case of state variable feedback which has been shown to be successful with a number of different structures, such as circular saws. Fukuda et al [22] have also shown the applicability of state variable feedback applied to torsional vibration in LSS.

A problem that arises in structures is their complexity, and the model describing the system contains unmodelled dynamics. State variable feedback does not necessarily address this issue, and other control techniques need to be employed. These are discussed briefly.

Probably the best known technique for poorly defined plants is the linear quadratic Gaussian (or LQG) control method. A number of papers have been published describing the process with which to follow if a LQG control solution is sought, one of those is the paper by Blelloch and Mingori [12]. In this paper the mathematics behind the LQG technique is discussed and the results for a complex antenna are

numerically presented. Other papers which discuss this approach are those by Czajkowski [19] and Belvin and Park [10]. Czajkowski, in addition to describing the LQG design approach, discusses the stabilisation of the spillover problem.

The quantitative feedback theory (QFT) for active vibration control is also presented by Yaniv and Horowitz [53]. Again, poorly defined plant parameters are necessary before the complexity of the QFT approach is to be justified. However, the disturbance uncertainty may be considered as the uncertainty of the plant and in doing so provide a basis for a QFT design. In this paper the difficulties of the LQG technique are referenced, and the results showing the suitability of QFT for active vibration control are presented.

Livneh and Slater [36] present an adaptive control approach to arbitrary excitations and unmodelled plant dynamics. As discussed in the paper for any plant with a completely defined dynamic model and a fixed set of parameters, the construction of a feedback control system will yield a stable response, generally conforming to the specifications of the system. The design difficulties present themselves when there is an uncertainty about the validity of the dynamic model of the plant. The authors of the paper then continue to develop the mathematical model of an adaptive control method, presenting numerical results of the response to a flutter model of an aeroelastic wind–tunnel model of a cantilever swept–back wing.

Another method whereby vibration may be reduced in structures is that presented by Morgül [43]. Here a specialised structure needs to be present for this technique to be useful, since a cantilevered beam is used, with a force and a torque applied to the free end. This force and torque are a function of the disturbance and are used in order that vibration be reduced within the beam.

In the research currently undertaken, these alternative control techniques used where the plant is not well defined are not of direct bearing to the scope of the research. However, another method that has only recently been documented, and is of more interest in the present research is the Modified Independent Modal Space Control (MIMSC) technique [7].

The MIMSC method, showing numerical and experimental results, was demonstrated by Baz and Poh [7]. A brief mathematical description of the MIMSC technique is outlined, describing the concept of spillover (further referred to in [13, 24, 19]). A flexible beam is used to experimentally illustrate the response of a beam to a given disturbance under the control of the MIMSC technique, with a comparison to the IMSC (or Independent Modal Space Control) method also being considered. The mathematical methods behind the MIMSC technique are more broadly presented in the paper by the same authors [8]. A further paper, again discussing the MIMSC method and its applicability to structural control, covering the same material was published the following year [9]. However, the complete mathematics describing the MIMSC method, and showing a closed form solution for the control constants was given by Meirovitch et al. [40, 41, 42]. These papers develop the governing equations for the MIMSC technique, then use a cost function to minimise force expended and vibration. From the minimisation of the cost function, the control constants are shown to be a function of the natural frequencies.

Baz and Poh [8] applied the technique to the use of the piezoelectric actuator by considering the effect of the bonding layer between the actuator and the beam to be controlled as well as an optimal position of the actuator. Although the MIMSC

method can be thought of as a time sharing technique, being able to employ more than one actuator, this paper considers only a single actuator and its optimal placement. A further paper discussing a numerical study of the MIMSC method for active control of vibrations of a cantilevered beam [18] was also presented at the conference on Recent Advances in Active Control of Sound and Vibration in April 1991.

A further control technique recently published is that regarding the theory of feedforward controlled system eigenproperties [15]. The purpose of this paper was to study the dynamics of a flexible structure with a feedforward control algorithm. In this paper the controlled system is shown to behave as having new eigenproperties, therefore having a different dynamic response. The eigenproperties are shown to be functions of the error sensor location and control force and independent of the input disturbance. This paper is also one of the first to discuss the experimental implementation of the control law using a digital controller.

Williams and Juang [52] considered pole/zero cancellation. State variable feedback is employed and cancellation of poles and zeros are carried out at specific points only. Hence, the closed-loop modes are unobservable at these points and therefore do not contribute to the measured response. Therefore, the dynamics expressed by the cancelled poles and zeros cannot be controlled, but do not contribute to the dynamic measured output response, and so the fastest possible exponential decay of the system to a disturbance is found. Since, any modes that decay slowly, but are not unstable and are not affected greatly by a control action may be cancelled to be unobservable in the measured output response. Then, the modes acted upon, that are affected greatly by a control action are forced to zero displacement as quickly as possible. In this research a collocation of sensors and actuators are employed, and numerical results are shown for three mass-spring-damper systems in series.

The background to the literature (section 3.2) indicates that many control techniques have been applied to the control of flexible structures. With the current research in this area new methods are being developed all the time. It is noticeable however that some techniques are more widely used than others. There are a number of reasons for this, and this chapter will outline a few of these reasons, before developing the mathematical background to the techniques that will be focussed on.

3.3 Feedback control

Almost all the control methods designed to control continuous systems use some form of feedback. Feedback is a process, whereby some or all of an output signal from an active device is sampled and fed back to the input in such a way as to either counteract or enhance the action of the original input signal. Intuitively, the feedback used in active vibration control should decrease if not negate the input signal to the structure. This is known as negative feedback.

Feedback has three main advantages when introduced into a control system.

- The first is in improvement in linearity of the system. This occurs because feedback causes the response of an active device to remain within close bounds of the set point. This, ensures the assumption of linearity around the set point is usually valid. Furthermore, linearity over the entire domain is improved with the use of feedback. This is clearly demonstrated by the addition of feedback

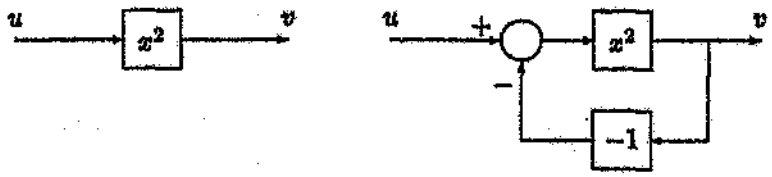

Figure 3.3: A scalar element with and without feedback.

on the scalar element, which is shown in Figure 3.3. The graphical results of the two block diagrams are shown in Figure 3.4, with the improvement of linearity clearly shown.

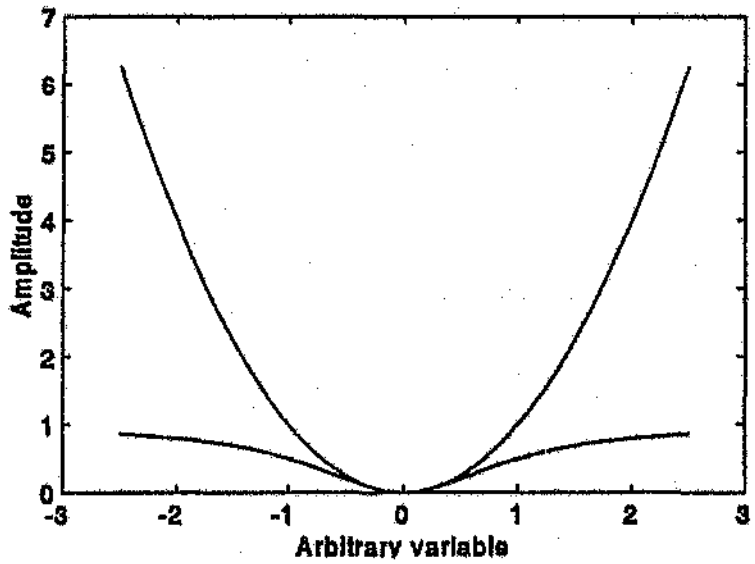

Figure 3.4: The plots of x^2 and $x^2/(x^2+1)$.

- A second advantage in using feedback control is the reduction in parameter sensitivity. This is an important factor when a plant parameter is calculated exactly, but is difficult to achieve in practice. Therefore, if the parameter sensitivity is reduced, a small change in plant parameters will not produce a large change in the dynamic response. Hence, plant parameters can be modelled as disturbances, and attenuation techniques can be applied to account for variations of system dynamics or parasitic effects.

3.4 Controlling continuous vibration

From the discussion of feedback control, it is evident that the feedback in a control system used in the reduction of structural vibration does present a number of advantages. Therefore, the control system must incorporate some type of feedback. Now, one of the simplest feedback control techniques must be that of state variable feedback control, which provides a suitable starting point of a structural vibration control law.

3.4.1 State variable feedback

State variable feedback is a technique whereby the states of the system are measured and used to modify either the actuating or control signal. The most prominent of the advantages of state variable feedback is that the system states contain a complete description of the plant dynamics. One of the main drawbacks of such a technique, is that in practise full state variable feedback is not generally used due to the cost of measurement equipment (sensors). Hence, one or more of the states is generally estimated. For example, if a number of accelerometers are used as the transducers, and velocity or effectively modal damping is needed to be fed back to the actuating signal, the signal from the sensor is numerically integrated. Therefore, the velocity state is estimated, and may not be as accurate a signal as if it were measured directly.

To demonstrate the use of state variable feedback, the governing equations are rewritten in terms of the state variables. For example, let the plant be described by the second order system

$$\ddot{x} + 2\zeta\omega\dot{x} + \omega^2 x = f(t) + f_d(t) \tag{3.1}$$

where $f_d(t)$ is a disturbance force. Rewriting $x = x_1$ and $\dot{x} = \dot{x}_1 = x_2$

$$\dot{x}_2 + 2\zeta\omega x_2 + \omega^2 x_1 = f(t) + f_d(t) \tag{3.2}$$

To modify the state variables, the force input to the actuator is chosen to be a combination of the state variables. For simplicity a linear combination is chosen. Therefore

$$f(t) = -(c_1 x_1 + c_2 x_2) \tag{3.3}$$

Equations 3.2 and 3.3 are combined to give

$$\dot{x}_2 + 2\zeta\omega x_2 + \omega^2 x_1 = f_d(t) \tag{3.4}$$

or

$$\dot{x}_2 + (2\zeta\omega + c_2)x_2 + (\omega^2 + c_1 x_1 = -(c_1 x_1 + c_2 x_2) + f_d(t) \tag{3.5}$$

Transforming equation 3.4 into the Laplace domain, and presenting it in the form of a transfer function, we obtain

$$X(s) = \frac{F_d(s)}{s^2 + (2\zeta\omega + c2)s + \omega^2 + c1} \tag{3.6}$$

From equation 3.6 the advantages of state variable feedback become evident. Both the states of the system may be altered independently, essentially increasing or decreasing stiffness and/or damping.

The numerator dynamics introduced with a technique such as PID control are not present, and therefore the increased amplitude of oscillation will not be present. In a different environment the use of integral action may be necessary to improve the steady-state performance of the system. However, the chance of overshoot due to the numerator dynamics for a structural vibration control problem is not worth the risk (it must be noted that in a system with different specifications the overshoot due to the presence of numerator dynamics may actually be desirable). In addition, the controller does not have to respond to possibly conflicting tasks simultaneously

(with both the derivative and integral action in the forward path). Furthermore, the derivative action in the forward loop as in PID control is also not present [46].

The above example demonstrates the applicability of state variable feedback to the task of vibration control. The two techniques used in this research employ state variable feedback, but because of the continuous system the models and hence controllers become more complex than discussed up to this point. Therefore, the first technique uses only a modification to the system damping and is known as direct velocity feedback. The second more complex technique is known as the Modified Independent Modal Space Control (MIMSC) method, and uses feedback of both stiffness and damping. These two methods are discussed further.

3.5 Direct velocity feedback

Recall that the governing equations for the cantilevered beam given in the principal or modal coordinates are of the form

$$\ddot{q}_1 + 2\zeta_1\omega_1\dot{q}_1 + \omega_1^2 q_1 = \frac{\phi_1^1}{2\omega_{d1}} f(t) \tag{3.7}$$

$$\ddot{q}_2 + 2\zeta_2\omega_2\dot{q}_2 + \omega_2^2 q_2 = \frac{\phi_1^2}{2\omega_{d2}} f(t) \tag{3.8}$$

$$\vdots$$

$$\ddot{q}_r + 2\zeta_r\omega_r\dot{q}_r + \omega_r^r q_r = \frac{\phi_1^r}{2\omega_{dr}} f(t) \tag{3.9}$$

As an example of the velocity feedback technique, consider a truncated model of the system incorporating the first two modes. Also, the voltage supplied to the actuator is directly proportional to the force (since the amplifier uses a current feedback module) and is denoted as $f(t) = kV(t)$. Therefore

$$\ddot{q}_1 + 2\zeta_1\omega_1\dot{q}_1 + \omega_1^2 q_1 = \frac{\phi_1^1}{2\omega_{d1}} kV(t) \tag{3.10}$$

$$\ddot{q}_2 + 2\zeta_2\omega_2\dot{q}_2 + \omega_2^2 q_2 = \frac{\phi_1^2}{2\omega_{d2}} kV(t) \tag{3.11}$$

In direct velocity feedback, velocity is fed back from two points on the beam and the resultant input voltage to the actuator is made a linear combination of these feedback signals

$$V(t) = c_1\dot{u}_1 + c_2\dot{u}_2 \tag{3.12}$$

As before the physical displacements and hence velocities are related to the modal coordinates as follows (note the truncation at the end of the second mode, due to the filtering of the input signal)

$$\dot{u}_1 = \phi_1^1\dot{q}_1 + \phi_1^2\dot{q}_2 \tag{3.13}$$

$$\dot{u}_2 = \phi_2^1\dot{q}_1 + \phi_2^2\dot{q}_2 \tag{3.14}$$

Combining equations 3.13 and 3.14 with equation 3.12

$$V(t) = (\phi_1^1 c_1 + \phi_2^1 c_2)\dot{q}_1 + (\phi_1^2 c_1 + \phi_2^2 c_2)\dot{q}_2 \tag{3.15}$$

Substituting equation 3.15 into equations 3.10 and 3.11

$$\ddot{q}_1 + 2\zeta_1\omega_1\dot{q}_1 + \omega_1^2 q_1 = \frac{\phi_1^1}{2\omega_{d1}} k\left[(\phi_1^1 c_1 + \phi_2^1 c_2)\dot{q}_1 + (\phi_1^2 c_1 + \phi_2^2 c_2)\dot{q}_2\right] \quad (3.16)$$

$$\ddot{q}_2 + 2\zeta_2\omega_2\dot{q}_2 + \omega_2^2 q_2 = \frac{\phi_1^2}{2\omega_{d2}} k\left[(\phi_1^1 c_1 + \phi_2^1 c_2)\dot{q}_1 + (\phi_1^2 c_1 + \phi_2^2 c_2)\dot{q}_2\right] \quad (3.17)$$

For simplicity introduce z_1 and z_2 where

$$z_1 = \phi_1^1 c_1 + \phi_2^1 c_2 \quad (3.18)$$

$$z_2 = \phi_1^2 c_1 + \phi_2^2 c_2 \quad (3.19)$$

Therefore, rewriting equations 3.16 and 3.17 in the simplified format

$$\ddot{q}_1 + 2\zeta_1\omega_1\dot{q}_1 + \omega_1^2 q_1 = \frac{\phi_1^1}{2\omega_{d1}} k(z_1\dot{q}_1 + z_2\dot{q}_2) \quad (3.20)$$

$$\ddot{q}_2 + 2\zeta_2\omega_2\dot{q}_2 + \omega_2^2 q_2 = \frac{\phi_1^2}{2\omega_{d2}} k(z_1\dot{q}_1 + z_2\dot{q}_2) \quad (3.21)$$

As can be seen from equations 3.20 and 3.21, coupling exists between the first and second modes (in fact if the input signal is not filtered correctly, this coupling exists to a greater or lesser extent between all the modes). This coupling between modes increases the complexity of the controller design and may even cause a reduction in system performance. However, the main concern with regard to modal coupling is that the higher order (or parasitic) modes which are not directly controlled may cause instability; this problem arises from a phenomenon known as spillover. For example, the governing equation of the third mode is given by

$$\ddot{q}_3 + 2\zeta_3\omega_3\dot{q}_3 + \omega_3^2 q_3 = \frac{\phi_3^3}{2\omega_{d3}} k(z_1\dot{q}_1 + z_2\dot{q}_2 + \cdots) \quad (3.22)$$

The third mode and all the other higher order modes are not being controlled. Now, let us say that the control action has been designed so that there is negative feedback on the first and second modes, ie. $\phi_1^1 z_1 < 0$ and $\phi_1^2 z_2 < 0$. If ϕ_1^3 has a different sign to one or both of ϕ_1^1 or ϕ_1^2, then positive feedback could arise on the third mode from the spillover of the control force from either or both modes one or two. Therefore, even for a small signal at the third mode frequency, the system response may be unstable.

In order to reduce the signals of the parasitic modes that influence the system response, the higher order modes on the signal received from the actuators is filtered out. The use of filters eliminates the spillover, and hence for a stable design guarantees stability of the entire plant if negative feedback exists on the first 2 modes of vibration. Digital filters are used in the practical part of this research and are discussed further in Chapter 5.

Since the truncated model can be made stable, the design of the direct velocity feedback technique must account for high order modes. However, it is necessary to demonstrate that to control n modes, n sensors along the beam must exist.

Consider the discrete model truncated to two modes

$$\ddot{q}_1 + 2\zeta_1\omega_1\dot{q}_1 + \omega_1^2 q_1 = \frac{\phi_1^1}{2\omega_{d1}} kV(t) \quad (3.23)$$

$$\ddot{q}_2 + 2\zeta_2\omega_2\dot{q}_2 + \omega_2^2 q_2 = \frac{\phi_1^2}{2\omega_{d2}} kV(t) \quad (3.24)$$

Suppose it is desired to control n modes of vibration. As before, the control voltage supplied to the actuator can be written as a linear combination of these feedback voltages

$$V(t) = c_1\dot{u}_1 + c_2\dot{u}_2 + \cdots + c_n\dot{u}_n \tag{3.25}$$

Thus in terms of the modal coordinates, the control voltage is

$$V(t) = \begin{bmatrix} c_1 & c_2 & \cdots & c_n \end{bmatrix} \begin{bmatrix} \phi_1^1 & \phi_1^2 & \cdots & \phi_1^r \\ \phi_2^1 & \phi_2^2 & \cdots & \phi_2^r \\ \vdots & \vdots & \ddots & \vdots \\ \phi_n^1 & \phi_n^2 & \cdots & \phi_n^r \end{bmatrix} \begin{Bmatrix} \dot{q}_1 \\ \dot{q}_2 \\ \vdots \\ \dot{q}_r \end{Bmatrix} \tag{3.26}$$

Using the notation of above and introducing a variable z, we have

$$V(t) = z_1\dot{q}_1 + z_2\dot{q}_2 + \cdots + z_r\dot{q}_r \tag{3.27}$$

where $z_1 = \phi_1^1 c_1 + \phi_2^1 c_2 + \cdots + \phi_n^1 c_n$
$z_2 = \phi_1^2 c_1 + \phi_2^2 c_2 + \cdots + \phi_n^2 c_n$
$\vdots$
$z_r = \phi_1^r c_1 + \phi_2^r c_2 + \cdots + \phi_n^r c_n$

Therefore, equations 3.20 and 3.21 become

$$\ddot{q}_1 + 2\zeta_1\omega_1\dot{q}_1 + \omega_1^2 q_1 = \frac{\phi_1^1}{2\omega_{d1}} k(z_1\dot{q}_1 + z_2\dot{q}_2 + \cdots + z_r\dot{q}_r) \tag{3.28}$$

$$\ddot{q}_2 + 2\zeta_2\omega_2\dot{q}_2 + \omega_2^2 q_2 = \frac{\phi_1^2}{2\omega_{d2}} k(z_1\dot{q}_1 + z_2\dot{q}_2 + \cdots + z_r\dot{q}_r) \tag{3.29}$$

Since feedback is being made from n points along the beam, $c_1, c_2, \cdots, c_n$ are selected in such a way as to develop negative feedback on the first n modes. The other terms contained in $z_{n+1} \cdots z_r$ cannot be determined using the n feedback points and are therefore considered uncontrollable modes. This shows that for direct velocity feedback to control n modes, at least n sensors are required.

3.5.1 Accounting for modal coupling

A number of techniques exist for dealing with the problem of modal coupling. Most methods try to reduce the amount of coupling between modes, however, this coupling cannot be completely eliminated.

If modal coupling could be eliminated completely, the controller complexity would be greatly reduced. This can be seen from equations 3.30 and 3.31. These equations are presented truncated to the first two modes, without modal coupling being present.

$$\ddot{q}_1 + 2\zeta_1\omega_1\dot{q}_1 + \omega_1^2 q_1 = \frac{\phi_1^1}{2\omega_{d1}} k\phi_1^1\dot{q}_1 \tag{3.30}$$

$$\ddot{q}_2 + 2\zeta_2\omega_2\dot{q}_2 + \omega_2^2 q_2 = \frac{\phi_1^2}{2\omega_{d2}} k\phi_2^2\dot{q}_2 \tag{3.31}$$

However, the uncoupled equations are not a true representation and therefore two more commonly used methods that reduce modal coupling are further outlined.

In the literature review, the technique of sensor placement was briefly discussed. One of the most important aspects of the sensor placement in flexible structures is directed at an attempt to reduce modal coupling. The sensors are placed so that they detect only one mode. This is impossible to achieve in practice, but for a limited number of modes, the sensors can be placed close to a point that aliase all but one mode of vibration. A second method that is employed in this research is the use of notch filters. By notch filtering the incoming signal from a sensor, all but one mode can be filtered out (it must be noted that the coupling cannot be eliminated completely, but is only reduced). The difficulty in this method is the expense of analogue filters, or the sampling speed required for the use of digital filters. The hardware needed to overcome these problems was acquired. The design of the notch filters and the selection of the control constants incorporating the effect of modal coupling is discussed further in Chapter 4.

3.6 MIMSC method

The Modified Independent Modal Space Control method uses a different approach to the problem of structural vibration compared to the velocity feedback method. Although this technique uses both velocity and position feedback, the modes remain uncoupled even when the force (or voltage) is applied to the beam via the actuator.

A more detailed model can be found in reference [9]. The governing equations are not truncated

$$\ddot{q}_r + 2\zeta_r\omega_r\dot{q}_r + \omega_r^2 q_r = \frac{\phi_i^r}{2\omega_{dr}} f(t) \tag{3.32}$$

where f is the modal force of the system. Writing equation 3.32 in terms of the physical force, leads to

$$\ddot{q}_r + 2\zeta_r\omega_r\dot{q}_r + \omega_r^2 q_r = \frac{\phi_i^r}{2\omega_{dr}} (\phi_r^r)^T F_r(t) \tag{3.33}$$

For convenience, the physical force applied to the beam through the actuator is denoted by $F(t)$.

From equations 3.32 and 3.33 it is evident that the modal and physical forces are related as follows

$$f = \phi^T F \tag{3.34}$$

The modal force can be written in two parts, the controlled part and the uncontrolled part, signified by the subscripts u and c. Expanding equation 3.34

$$[f] = \begin{Bmatrix} f_c \\ f_u \end{Bmatrix} = \left[\begin{array}{ccc|ccc} \phi_1^1 & \cdots & \phi_1^n & \phi_1^{n+1} & \cdots & \phi_1^r \\ \vdots & \ddots & \vdots & \vdots & \ddots & \vdots \\ \phi_n^1 & \cdots & \phi_n^n & \phi_n^{n+1} & \cdots & \phi_n^r \\ \hline \phi_{n+1}^1 & \cdots & \phi_{n+1}^n & \phi_{n+1}^{n+1} & \cdots & \phi_{n+1}^r \\ \vdots & \ddots & \vdots & \vdots & \ddots & \vdots \\ \phi_r^1 & \cdots & \phi_r^n & \phi_r^{n+1} & \cdots & \phi_r^r \end{array}\right]^T \begin{Bmatrix} F_c \\ F_u \end{Bmatrix} \tag{3.35}$$

Applying the transpose in equation 3.35, results in

$$[f] = \begin{Bmatrix} f_c \\ f_u \end{Bmatrix} = \left[\begin{array}{ccc|ccc} \phi_1^1 & \cdots & \phi_n^1 & \phi_{n+1}^1 & \cdots & \phi_r^1 \\ \vdots & \ddots & \vdots & \vdots & \ddots & \vdots \\ \phi_1^n & \cdots & \phi_n^n & \phi_{n+1}^n & \cdots & \phi_r^n \\ \hline \phi_1^{n+1} & \cdots & \phi_n^{n+1} & \phi_{n+1}^{n+1} & \cdots & \phi_r^{n+1} \\ \vdots & \ddots & \vdots & \vdots & \ddots & \vdots \\ \phi_1^r & \cdots & \phi_n^r & \phi_{n+1}^r & \cdots & \phi_r^r \end{array}\right] \begin{Bmatrix} F_c \\ F_u \end{Bmatrix} \tag{3.36}$$

Equation 3.36 can be written as follows

$$\begin{Bmatrix} f_c \\ f_u \end{Bmatrix} = \begin{bmatrix} B_{cc} & B_{cu} \\ B_{uc} & B_{uu} \end{bmatrix} \begin{Bmatrix} F_c \\ F_u \end{Bmatrix} \tag{3.37}$$

Now, if n control actions and n sensors are present on the beam, F_u becomes zero. Therefore, equation 3.37 reduces to

$$f_c = B_{cc} F_c \tag{3.38}$$

and (3.39)

$$f_u = B_{uc} F_c \tag{3.40}$$

Hence, the force that excites the uncontrolled modes (also known as residual or spillover modes) is written as a function of the controlled physical force. In turn the uncontrolled modal force can be shown to be a function of the controlled modal force [40, 41, 42]. This allows the determination of the physical value of the uncontrolled modal force, which was assumed to be zero by the IMSC [7].

As stated previously the MIMSC technique employs feedback on both the velocity and position vectors and it can be shown that the modal control force has the form [40]

$$f_r = -\frac{1}{R}(g_{1,r}\omega_r q_r + g_{2,r}\dot{q}_r) \tag{3.41}$$

where $g_{1,r}$ and $g_{2,r}$ are the position and velocity control constants respectively for mode r and

R is a factor that weighs the importance of minimising the vibration compared to the expenditure of the control force.

Now, to determine the control gains g_1 and g_2, set up a performance index that is minimised subject to equation 3.32. This is the same technique that will be applied in Chapter 4 in order to determine the control constants for the direct velocity feedback technique. However, the optimisation for the velocity feedback will be carried out numerically. Meirovitch and co-workers [40, 41, 42], have developed a closed form solution to the problem

$$\text{MIN} \quad J = \int_0^\infty \left[(\omega_r^2 q_r^2 + \dot{q}_r^2) + (R f_r^2)\right] dt \tag{3.42}$$

and showed the control gains to be

$$g_{1_r} = -\omega_r R + \sqrt{(\omega_r R)^2 + \omega_r^2 R} \tag{3.43}$$

and (3.44)

$$g_{2_r} = \sqrt{2R\omega_r\left(-\omega_r R + \sqrt{(\omega_r R)^2 + \omega_r^2 R}\right) + \omega_r^2 R} \text{ or} \tag{3.45}$$

A further strategy developed in conjunction with the MIMSC method is a unique time sharing mechanism whereby a small number of actuators can be used to control a large number of modes. In this strategy the modes are ranked according to their modal energy at any time instant. This modal energy is given by

$$E = \omega_r^2 q_r^2 + \dot{q}_r^2 \tag{3.46}$$

where the $\omega_r^2 q_r^2$ forms the potential energy part and $\dot{q}_r^2$ forms the kinetic energy part. Then the actuator is dedicated to controlling that mode with the most modal energy, until a second signal is received (the next sample). If more than one actuator exists, the second actuator is dedicated to the mode with the second most modal energy and so forth.

As discussed, the spillover force which is not zero, may be written in terms of the controlled modal force, denoted by f_c. If, however, the input signal is filtered, the spillover forces generated will have very little or no effect, but if no filters are present spillover forces can be determined numerically. This allows one to determine the effect of the spillover forces and perhaps even necessitate the use of the actuator in controlling a mode that was not initially intended to be controlled. Furthermore, the spillover forces may actually improve the performance of the controller by providing negative feedback on some or all of the parasitic modes.

Chapter 4

Application of Control to the Beam

The two control techniques discussed in Chapter 3 are applied to the beam. The simulations are constructed in SIMULINK, running on MATLAB. Both the governing equations of the cantilevered beam and of the control algorithm are entered in the form of a block diagram. Therefore the block diagram form of the differential equations governing the cantilevered beam are presented. Once these have been developed, the dynamic response of the beam to an input disturbance can be shown, and compared with the uncontrolled response to the same input.

4.1 Uncontrolled response of the cantilevered beam

A method of visualising the system of equations that govern the cantilevered beam, including the direct velocity feedback control algorithm is to represent the ordinary differential equations in terms of a block diagram. The block diagram of the uncontrolled response is developed here, so as to give a basis against which the responses of the beam including the control laws can be compared.

4.1.1 The block diagram of the cantilevered beam

From section 2.3 the mathematical model governing the cantilevered beam was given as

$$\ddot{q}_1 + 2\zeta_1\omega_1\dot{q}_1 + \omega_1^2 q_1 = \frac{\phi_1^1}{2\omega_{d1}} f(t) \tag{4.1}$$

$$\ddot{q}_2 + 2\zeta_2\omega_2\dot{q}_2 + \omega_2^2 q_2 = \frac{\phi_1^2}{2\omega_{d2}} f(t) \tag{4.2}$$

Using equations 4.1 and 4.2, a block diagram was constructed so that the simulated response of the cantilevered beam to an input could be determined. The block diagram is given in Figure 4.1. In Figure 4.1 u_1 and u_2 represent the physical displacement of the beam at two different physical positions along the beam. These two positions as mentioned earlier are 117mm and 300mm from the base of the beam respectively. These positions are also be referred to as positions one and two throughout the text. The input force F_{dist} is a physical force.

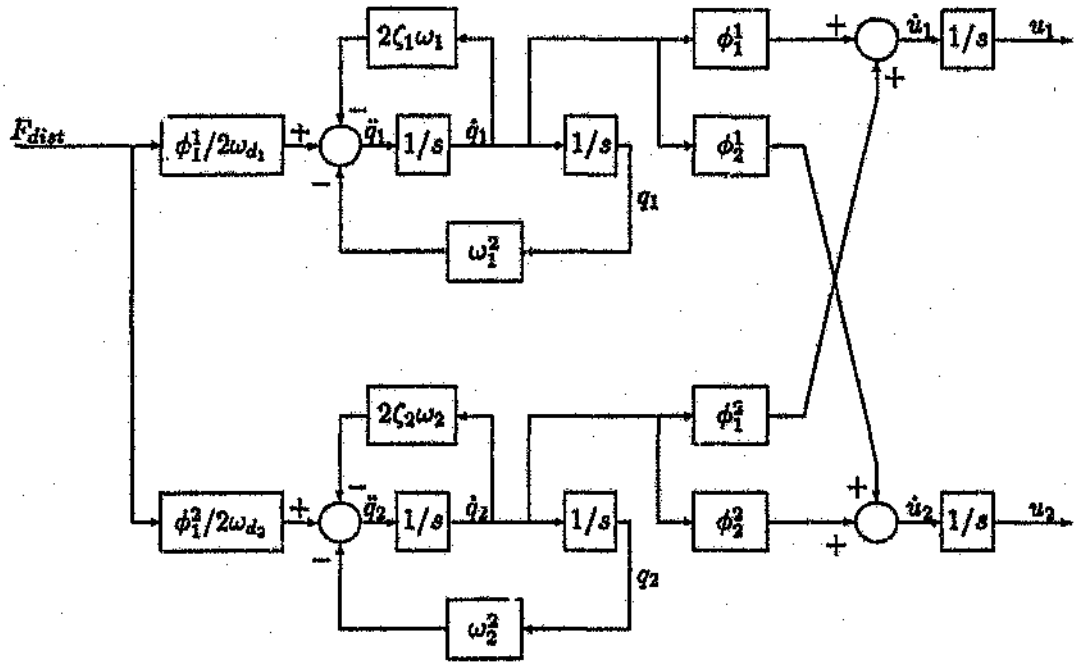

Figure 4.1: The block diagram showing the uncontrolled dynamics.

4.1.2 Forced response

The basis used for comparison is a pulse force input. This pulse is generated from a finite force input at time zero over a finite time span (which can be set to a fraction of a second). The actual magnitude of the input force disturbance was chosen such that a physical meaningful displacement of the beam would occur.

Although, the pulse is essentially a numerical forcing function, it presents a good comparison between dynamic responses for different systems. Furthermore, the numerical pulse may be favourably compared to the action of the experimental impulse hammer. The pulse force input also excites of a broad frequency band. Therefore, many resonances are simultaneously excited, providing for a better test of the control techniques.

The impulse force may be mathematically represented by

$$u = \begin{cases} 1 & t = 0 \\ 0 & t > 0 \end{cases} \tag{4.3}$$

where u is vertical displacement and t is time. This demonstrates that the impulse force is a convenient forcing function for analysis of the response of the structure. This is true because after time zero (or in practical applications after a short time period) the forcing function is no longer present and does not interfere with the response of the structure which may then be directly analysed.

The response of the cantilevered beam to the pulse disturbance at time zero without any structural vibration control is shown in Figures 4.2 and 4.3.

The responses given in Figures 4.2 and 4.3 are the physical displacements at each of the two positions along the beam. The physical displacements are made up of

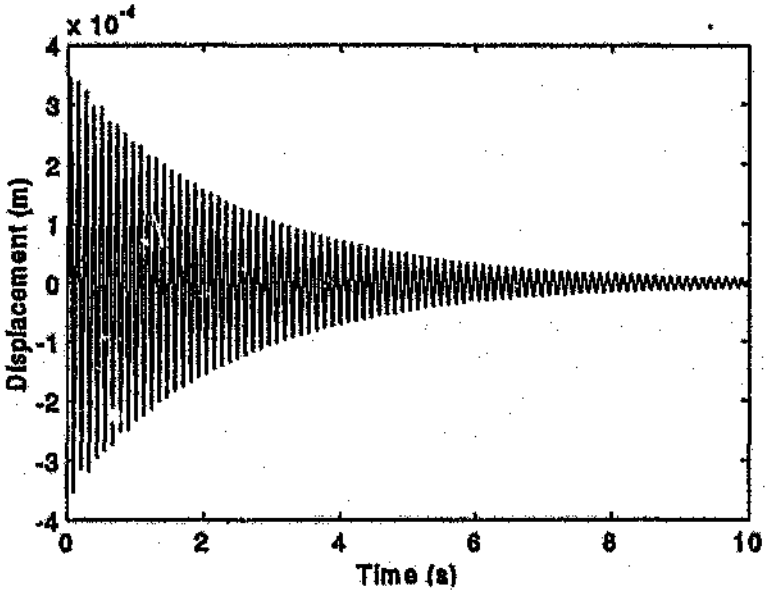

Figure 4.2: Uncontrolled response at position 1.

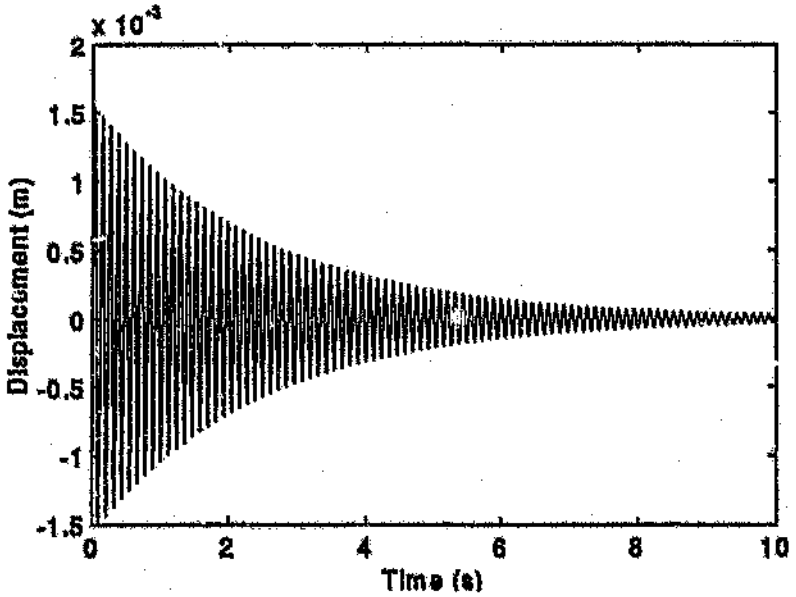

Figure 4.3: Uncontrolled response at position 2.

a combination of the modal displacements q_1 and q_2. In addition the true value of displacement should be noted, since the magnitude of the input disturbance is set such that physically meaningful results are obtained.

Although, in practice the uncontrolled decay of the dynamic response of the cantilevered beam is made up of infinitely many modal displacements, the truncation to the first two modes gives a fairly good comparison to that which is found in practice. This is especially true in large mechanical structures where it is often found that lower order modes, if not only the first mode, is of any consequence. This is known as the dominant root approximation.

4.2 Direct velocity feedback

As discussed in section 3.5, due to the limitation of the digital controller, only two modes could be controlled by this method. Therefore, as presented in Chapter 3 the mathematical model is truncated to two modes. In addition, the filtering and signal conditioning are part of the control algorithm and can be ignored.

4.2.1 Block diagram

The truncated two mode mathematical model in terms of modal coordinates, including the control action is

$$\ddot{q}_1 + 2\zeta_1\omega_1\dot{q}_1 + \omega_1^2 q_1 = \frac{\phi_1^1}{2\omega_{d_1}} k\left[(\phi_1^1 c_1 + \phi_2^1 c_2)\dot{q}_1 + (\phi_1^2 c_1 + \phi_2^2 c_2)\dot{q}_2\right] \quad (4.4)$$

$$\ddot{q}_2 + 2\zeta_2\omega_2\dot{q}_2 + \omega_2^2 q_2 = \frac{\phi_1^2}{2\omega_{d_2}} k\left[(\phi_1^1 c_1 + \phi_2^1 c_2)\dot{q}_1 + (\phi_1^2 c_1 + \phi_2^2 c_2)\dot{q}_2\right] \quad (4.5)$$

These equations can be presented in terms of the control voltage V as

$$\ddot{q}_1 + 2\zeta_1\omega_1\dot{q}_1 + \omega_1^2 q_1 = \frac{\phi_1^1}{2\omega_{d_1}} kV(t) \quad (4.6)$$

$$\ddot{q}_2 + 2\zeta_2\omega_2\dot{q}_2 + \omega_2^2 q_2 = \frac{\phi_1^2}{2\omega_{d_2}} kV(t) \quad (4.7)$$

where

$$V(t) = c_1\dot{u}_1 + c_2\dot{u}_2 \quad (4.8)$$

The physical velocities are related to the modal coordinates as follows

$$\dot{u}_1 = \phi_1^1\dot{q}_1 + \phi_1^2\dot{q}_2 \quad (4.9)$$

$$\dot{u}_2 = \phi_2^1\dot{q}_1 + \phi_2^2\dot{q}_2 \quad (4.10)$$

The block diagram representing these equations is given in Figure 4.4. Note that both the physical and modal states of the cantilevered beam are easily extracted and consequently can be dynamically monitored.

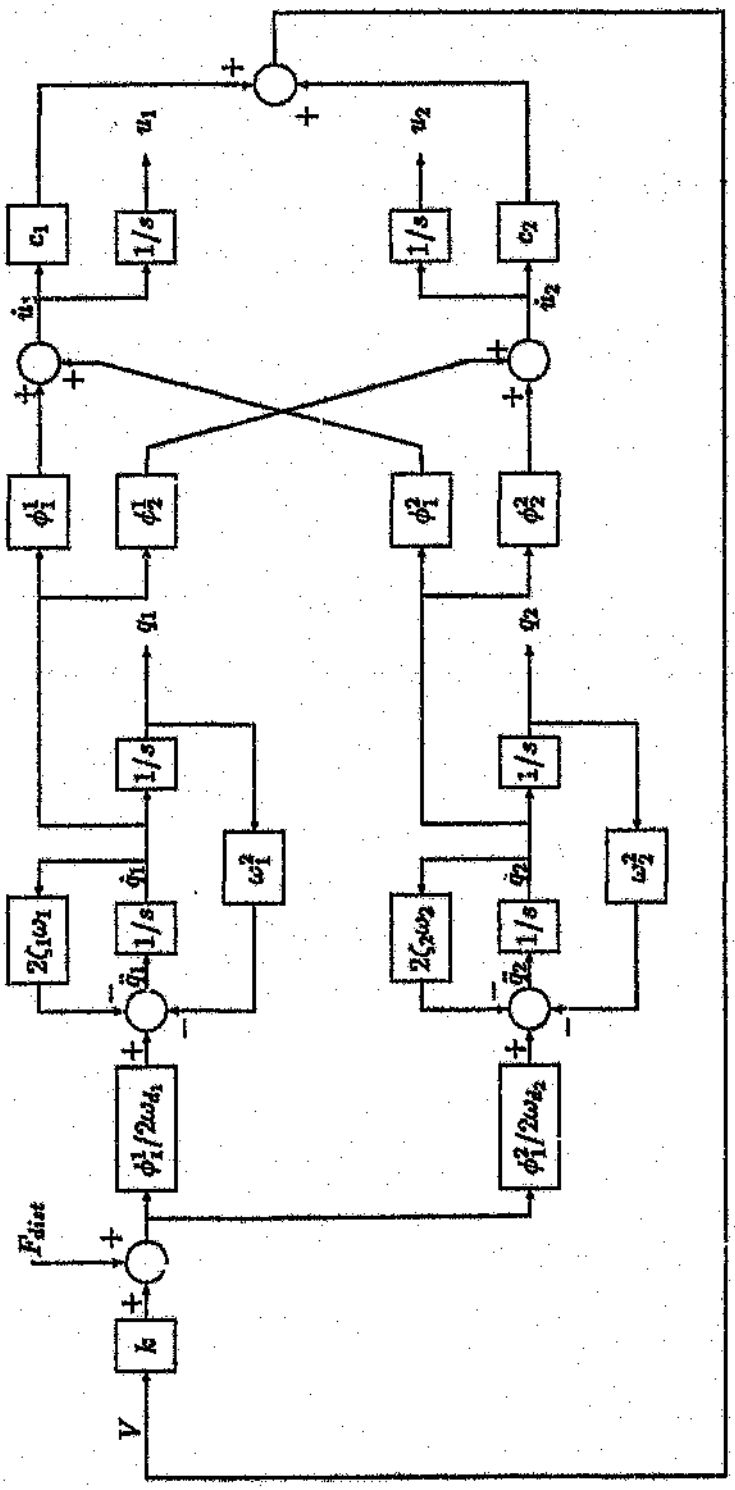

Figure 4.4: The block diagram for velocity feedback control law.

4.2.2 Control constant determination

As can be seen from Figure 4.4 no numerical values are given, and the control constants are denoted as c_1 and c_2. The only unknowns are therefore the disturbance input and the control constants. It has been decided to use a pulse input disturbance that is large enough to give an initial displacement of a suitable physical size (this is applied at the same point as the actuator), and the control constants will be determined using an optimisation process.

It must be noted that these control constants are specific to the type of force disturbance and if one had to choose a different input, the control constants would then be suited for that particular setup.

In order to determine the best control constants for the pulse disturbance, it must be decided exactly what the aim of the vibration control is. Possible alternatives are

- An initial reduction in physical displacement, but allowing the beam to still oscillate as per the open loop system.
- Not as stringent a control on the initial displacement but reducing the oscillatory behaviour of the open loop system.
- Conserving energy applied to the structure, which in turn does not present as good a solution when the main aim is to eliminate the vibration as quickly as possible.

It was decided to use the second option, since trying to control the initial displacement would tend to overload the actuator.

Therefore, an objective function was setup to reflect this decision. The other point that must be included in the objective function is the limit on the physical voltage that can be supplied to the actuator. Once the objective function is setup to incorporate these issues, this function is then minimised to determine the control constants that best suit this specific application.

The main aim of the optimisation is to minimise the physical displacement, or in mathematical terms

$$\lim_{t\to\infty} (|u_1| + |u_2|) = 0 \tag{4.11}$$

Note that a square function of u may be used, as opposed to the absolute value function. Now to make sure that the importance of reducing the physical displacement is enhanced (as discussed above), the absolute value of the displacement and voltage functions is weighted by multiplying each with a function of time. The positive part of the straight line $y = x$ was initially used as the time function, but it was found that the best results were obtained by multiplying the absolute value functions by a function where each time step is raised to the power of a quarter.

$$y = t_0^{1/4} + t_1^{1/4} + \cdots t_{t_n}^{1/4} \tag{4.12}$$

where t_n denotes the last time step.

Therefore from equation 4.11

$$\lim_{t\to\infty} (y|u_1| + y|u_2|) = 0 \tag{4.13}$$

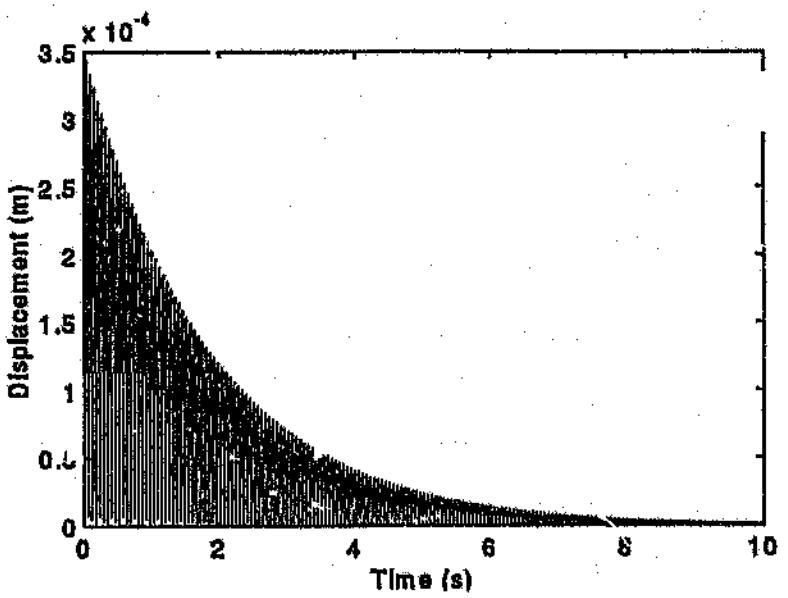

Figure 4.5: A plot of the absolute value of the physical displacement.

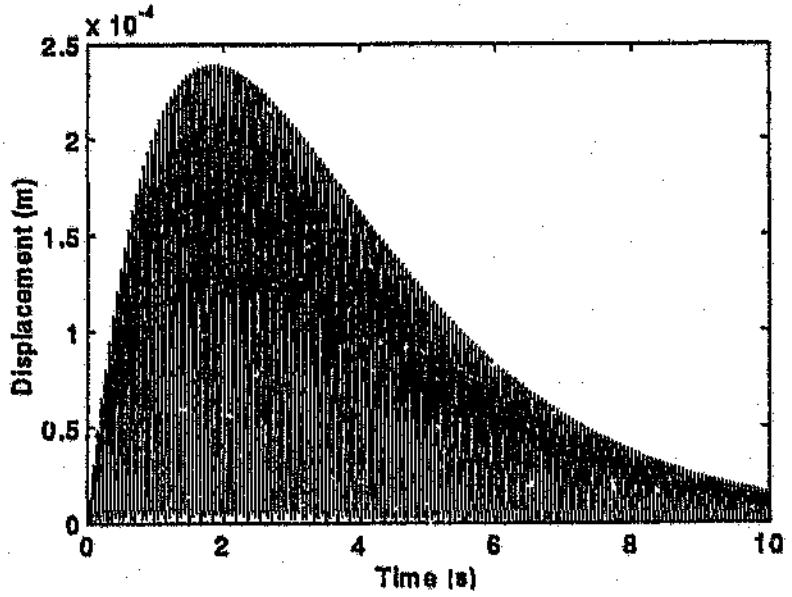

Figure 4.6: A plot of the absolute value of the physical displacement multiplied through by the time function y.

The effect of multiplying through by a function of this nature is clearly shown by comparing Figures 4.5 and 4.6. Figure ' . a plot of the absolute value of one of the physical displacements, compared v gure 4.6 which is the absolute value of a physical displacement multiplied through by the function given in equation 4.12. It is clear from these two figures that the importance of reducing the vibration is enhanced as time progresses.

Writing this as an objective function, J to be minimised gives

$$J = \int_0^\infty (yw_1|u_1| + yw_2|u_2|)\,dt \tag{4.14}$$

where w_1 and w_2 are weighting constants chosen so that approximately equal weighting is given to both the physical displacements.

At this point the contribution of the voltage is incorporated, and therefore equation 4.14 becomes

$$J = \int_0^\infty (yw_1|u_1| + yw_2|u_2| + yw_3|V|)\,dt \tag{4.15}$$

where w_3 is consistent with the weighting constants w_1 and w_2.

It must be noted that by chang. the values of the weighting constants, different results are obtained and a suitable solution can be obtained after many iterations.

The direct velocity feedback system in Figure 4.4 together with the objective function (equation 4.15) results in a constrained optimisation problem which was solved using MATLAB. The main constraint is the physical voltage that can be applied to the actuator; which is set at a maximum of 10 volts. The constrained optimisation algorithm determines the minimum of the objective function and the corresponding control constants by iteration.

Various control constants were found depending on the initial guess. The best solution for the specified problem was found to be where $c_1 = -54.6$ and $c_2 = -2360.0$.

It is interesting to note how the objective function varies according to the change in control constants. Therefore, the plot of the objective function J (on the z-axis) versus c_1 on the x-axis and c_2 on the y-axis is given in Figure 4.7. In Figure 4.7, c_1 is varied from -200 to 200 in steps of 20 and c_2 is varied from -4000 to 3000 in steps of 50. For this figure to be more meaningful, a plot of the change of voltage with respect to the control constants must also be considered. This is true, since, a constrained optimisation is used, with the constraint on the maximum voltage. The optimisation is done, so that all values of voltage less than or equal to zero are allowed. Figure 4.8 shows a plot of the voltage versus the control constants, with the voltage values that are not allowed set to zero. This shows on the pl as part of the zero voltage plane. Since these particular values of control constant are not allowed, the corresponding values in Figure 4.7 are also set to zero, indicating the minimum of the jective function clearly. The axes and values in Figure 4.8 are consistent with those in Figure 4.7.

4.2.3 Controlled response

Using the block diagram in Figure 4.4, together with the modal parameters experimentally determined and the control constants given in section 2.2.3, the forced

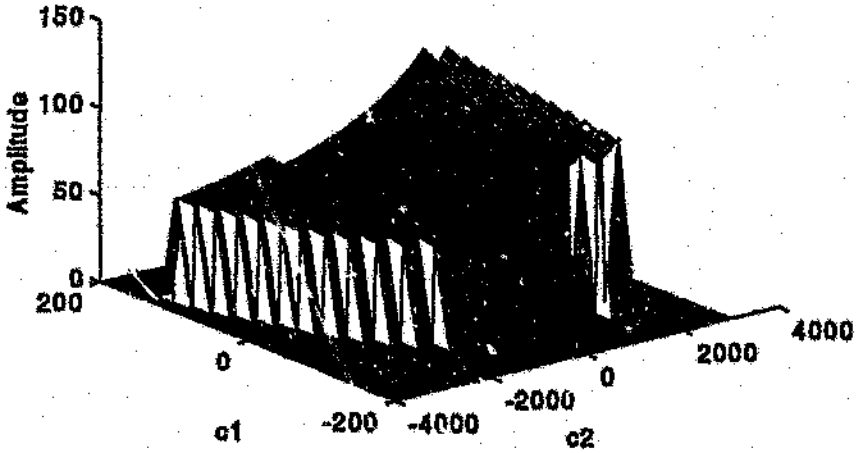

Figure 4.7: A plot of the objective function versus control constants.

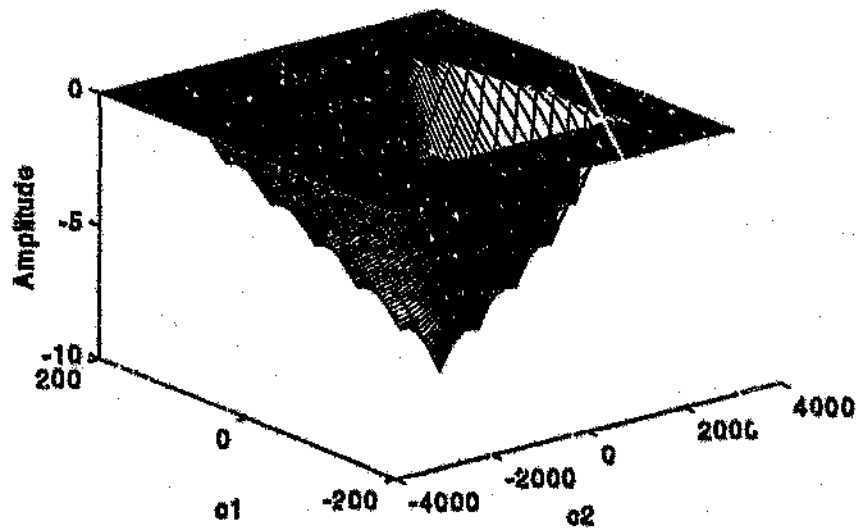

Figure 4.8: A plot of voltage versus the control constants.

response due to a pulse input was determined. Figures 4.9 and 4.10 show the displacement due to the controlled forced response at positions 1 and 2 respectively and Figure 4.11 shows the voltage applied to the actuator. In addition Figure 4.12 is also included to show the difference in the voltage against time plot for a different approach namely that of trying to reduce the initial amplitude of vibration, but not attempting to reduce the oscillatory behaviour thereafter.

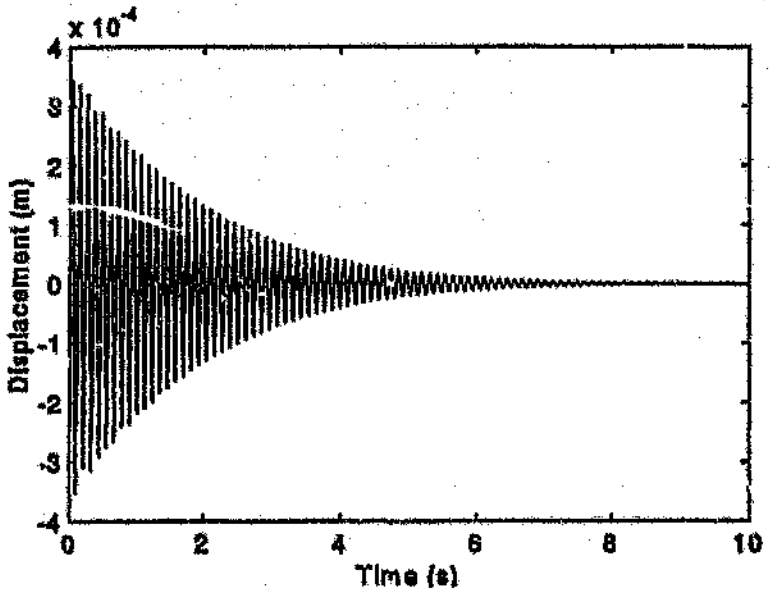

Figure 4.9: Controlled forced response at position 1.

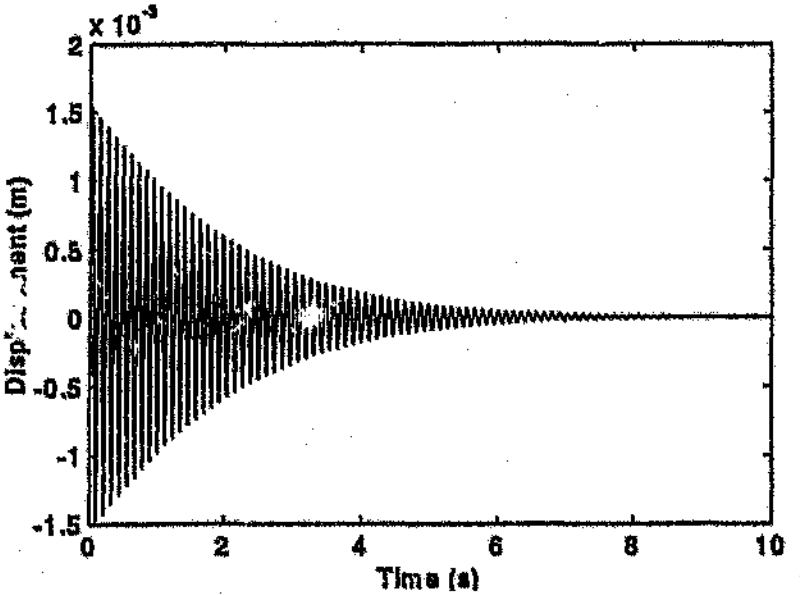

Figure 4.10: Controlled forced response at position 2.

The actuator limited the avaliable force to control the vibrating beam. Therefore,

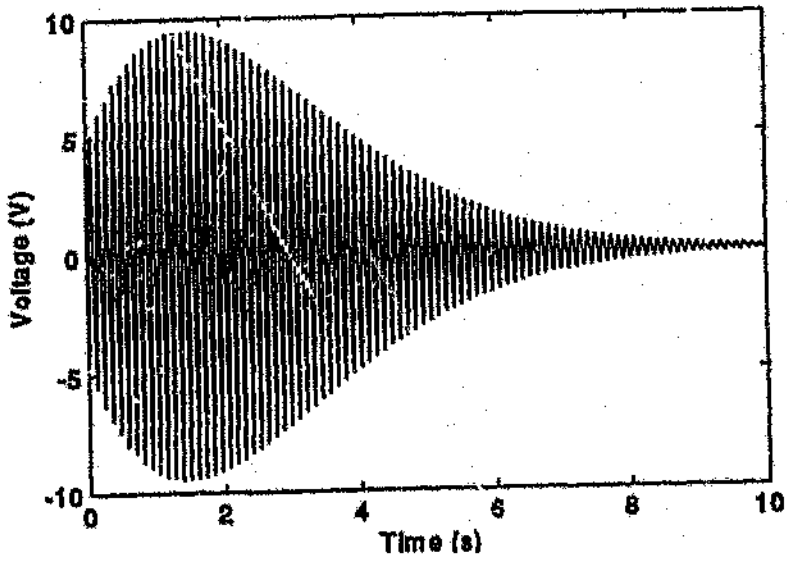

Figure 4.11: Voltage applied to the actuator.

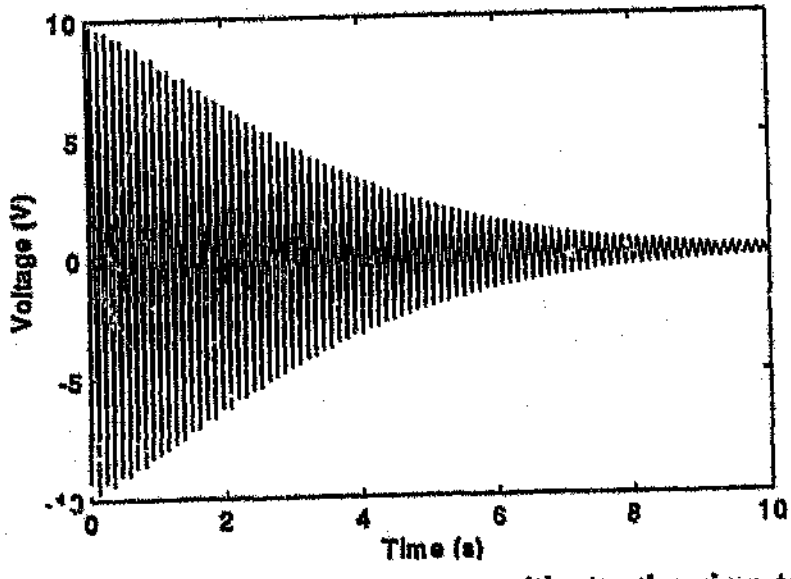

Figure 4.12: Voltage applied to the actuator with attention given to the initial displacement.

a large improvement over the uncontrolled beam is not found.

4.3 MIMSC method

The MIMSC method attempts to control a number of modes, with a reduced number of actuators. This is done by a time sharing method and ranking the modes according to the modal energy. For this reason, more than two modes could be attempted to be controlled using the single actuator. Therefore, the following discussion shows the response of the system using the MIMSC method attempting to control the first three modes. As before the signal conditioning and filtering to achieve this practically is assumed to be present on the input and output signals.

4.3.1 Block diagram

The simulation of the MIMSC technique was done using SIMULINK, which requires a block diagram to be entered into the package. Recalling the governing equations of the cantilevered beam are

$$\ddot{q}_r + 2\zeta_r\omega_r\dot{q}_r + \omega_r^2 q_r = \frac{\phi_1^r}{2\omega_{d_r}}\phi_r^r f_r(t) \tag{4.16}$$

Furthermore, the modal force is a function of both the modal velocity and displacement and is represented by

$$f_r = -\frac{1}{R}(g_{1_r}\omega_r q_r + g_{2_r}\dot{q}_r) \tag{4.17}$$

Another consideration when developing a control system for the MIMSC technique, is the time–sharing mechanism used to share the actuator between a number of modes. As discussed this is done by ranking the modes due to modal energy given by

$$E = \omega_r^2 q_r^2 + \dot{q}_r^2 \tag{4.18}$$

From the above equations we can construct the block diagram for the MIMSC method, so that a numerical result to the problem may be found. The block diagram depicting the model of the cantilevered beam and the control technique is given in Figure 4.13. The block diagram depicted in Figure 4.13 is truncated at the third mode. The first three modes are used as an example to show that the time sharing mechanism allows control to be placed on more modes with a fewer number of actuators.

In Figure 4.13, the block labelled 'Function' is where the simulation package computes which mode has the highest modal energy at that instant. Hence, the output of physical force (applied to the actuator) is determined with relation to the modal energy and fed back to be summed with the disturbance force.

4.3.2 Controlled response

The controlled response for a pulse input disturbance (consistent with the input for the direct velocity feedback technique) is given in Figure 4.14 for position one along the beam. The voltage applied to the actuator is also shown in Figure 4.15.

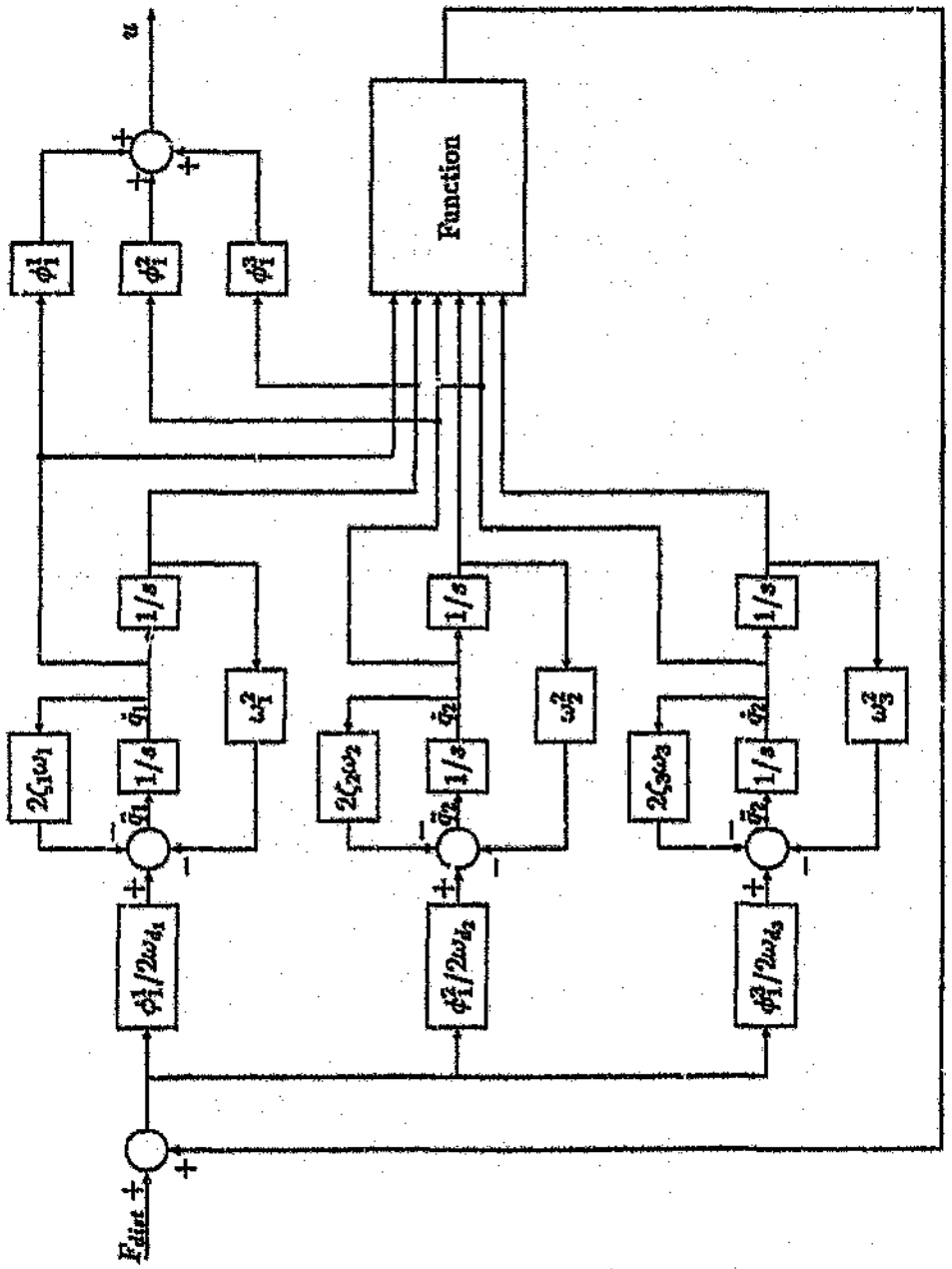

Figure 4.13: Block diagram for the MIMSC method.

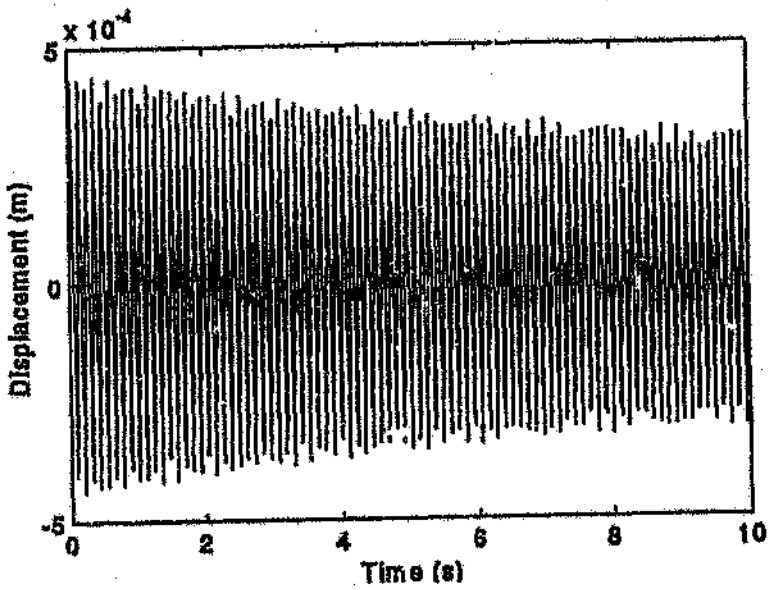

Figure 4.14: Controlled response at position 1, using the MIMSC method.

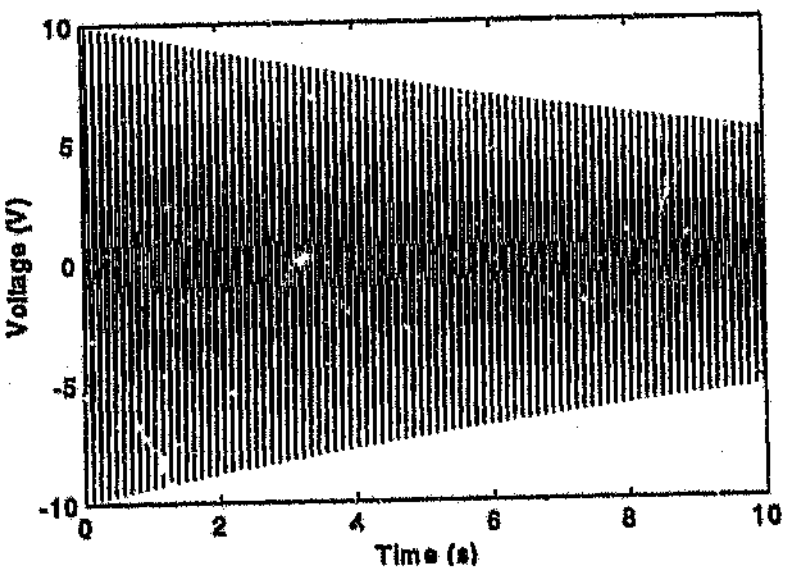

Figure 4.15: Voltage applied to the actuator for the controlled response, using the MIMSC method.

It is evident from Figures 4.14 and 4.15 that the use of the MIMSC method for the particular input disturbance given is worthless (the axes on Figure 4.14 are not the same as those previously shown in the free response). In fact the natural decay of the system shows a better dynamic response than with the inclusion of the control method. As before, if the limit on actuation energy was not as stringent, a stable quicker exponential decay of the vibration could be found.

To demonstrate the load placed on the actuator by the MIMSC method, a different set of solutions is presented. This solution is determined for the system having a pulse input disturbance of magnitude twenty times less than that previously used. Figure 4.16 shows the response of the cantilevered beam for the disturbance discussed, while Figure 4.17 shows the corresponding use of voltage by the actuator.

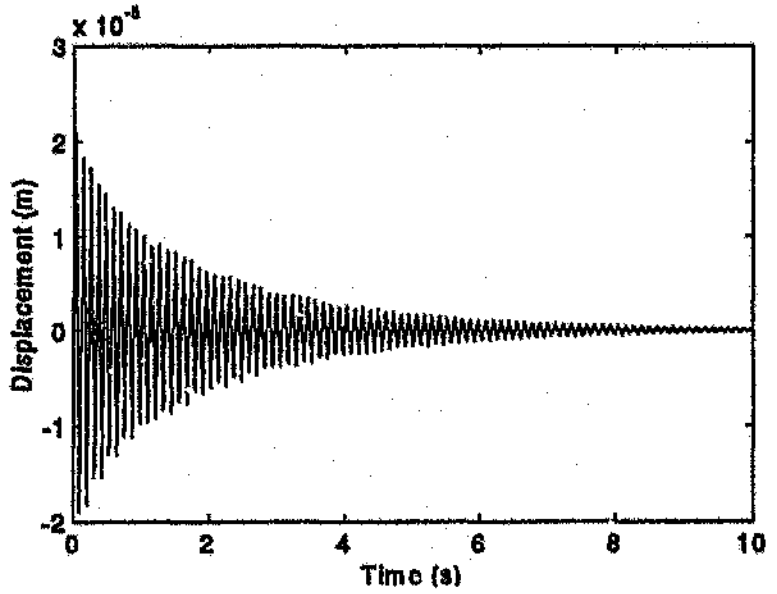

Figure 4.16: Controlled response at position 1, using the MIMSC method with a smaller magnitude disturbance.

4.4 Discussion

By comparing the graphs that have been presented in this chapter, it is evident that the reduction in vibration over a long time period is only marginal or non-existent with the addition of a vibration control method, with the initial conditions as previously stated.

The other point that is of significance and is shown clearly in the discussion of the direct velocity feedback technique and the MIMSC method is the limit on force that can physically be applied to the beam. This is due to the limits of the signal conditioners and the actuator itself. It therefore becomes an important factor to note when developing a control system, since a far more impressive dynamic response will be found without the physical limits of the actuator. This is illustrated in

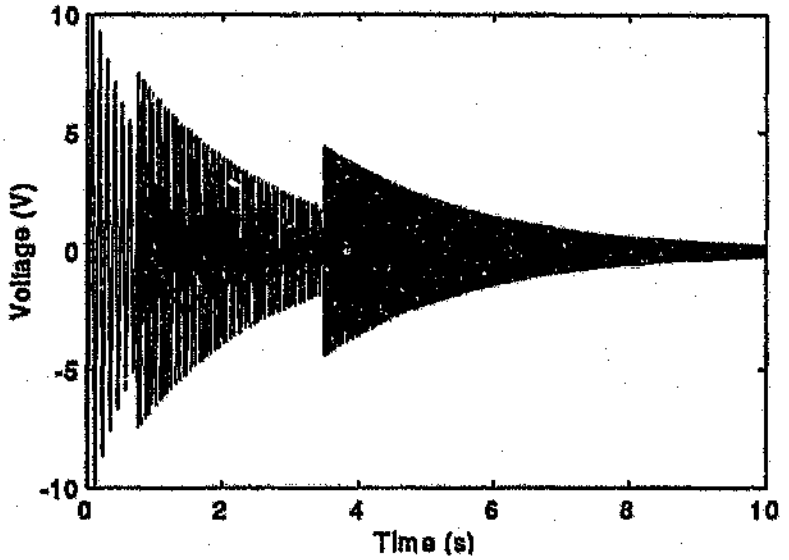

Figure 4.17: Voltage applied to the actuator for the controlled response, using the MIMSC method with a smaller magnitude disturbance.

Figures 4.16 and 4.17. Although, these figures are obtained with the use of the MIMSC technique, a similar dynamic response of the beam will be obtained using the direct velocity feedback method.

4.4.1 Direct velocity feedback vs. MIMSC

These two techniques are both based on the same principal, namely state variable feedback. However, the MIMSC method employs both position and velocity feedback, while the direct velocity feedback method uses only velocity feedback. It is important to note that neither of these methods use true state variable feedback, since accelerometers are used and the velocity and position of the beam are estimated. In the case of the MIMSC method a double integrator is used to determine the physical position of the beam. This makes the MIMSC technique more complex and intuitively suggests that it should solve the problem better provided that the states measured and synthesised are an accurate representation of the physical behaviour. However, it must be realised, that with the added complexity of the control system, the time to calculate the actuator force is increased and hence the time delay between the samples is increased. The effect can negate the intuitive feel that the MIMSC method should perform better than the velocity feedback method for the same system.

There is a further difference between the two methods presented in this dissertation, however this is more of a philosophy than part of the control technique developed. This difference is the time sharing mechanism implemented by the MIMSC method. Since the time sharing is built around the state variable feedback control it is not strictly part of the control technique, but rather an addition to the overall control system, incorporated in an attempt to control many modes with a fewer number of actuators. One may view this as a primitive adaptive control strategy.

By studying the plots representing the dynamic response of the controlled system, it is evident that the MIMSC method uses more energy to achieve the same result. This does not confirm the suspicion that by using both velocity and position feedback, the dynamics of a structure may be better controlled than by simply using velocity feedback. Numerically this is easily shown and may be enhanced in the physical implementation, since the complexity of the control method may challenge the controller and actuator further, resulting in a poorer dynamic response than that represented in the numerical solution. The experimental implementation and results are presented in the next chapter.

A further point that must be discussed is the evident time sharing mechanism of the MIMSC method. This can be seen from the plot showing voltage versus time with the MIMSC control method in operation (Figure 4.17). The actuator is dedicated to a certain mode and the change from controlling the first mode to the second mode and third is clearly seen. It is also clear that when too demanding a task is placed on the controller, an attempt to control only the first mode is made. Again this can be seen from one of the plots representing voltage versus time with the MIMSC method in operation (Figure 4.15).

In this section the two control methods are compared, but the direct velocity feedback method is designed to control the first two modes, while the MIMSC method is shown to attempt to control the first three modes of vibration. In fact it makes little or no difference to the dynamic response of the cantilevered beam if the MIMSC method is dedicated to only the first two modes. This is true since the major initial task of the control system is to damp out the intense vibration caused by the first mode of vibration. This is again clearly seen in the figures describing the voltage supplied to the actuator for the MIMSC method.

Chapter 5

Experimental overview and results

5.1 Experimental set-up

As discussed throughout this dissertation, the experimental apparatus used to examine structural vibration control was a steel cantilevered beam. This beam is made from spring steel to provide flexibility and is clamped between two mild steel brackets, so as to simulate a fixed end as closely as possible. The dimensions of the beam were chosen so that the length of the beam was very much greater than its thickness. This allowed for the assumptions made in Chapter 2 to hold true. The dimensions and mechanical properties of the spring steel beam are given in Table 5.1, whilst Figure 5.1 describes the cantilevered beam graphically, showing the dimensions used.

Length (mm)	Thickness (mm)	Width (mm)	Youngs Modulus (GPa)	Density (kg/m^3)
400.0	1.6	31.5	207	7600

Table 5.1: Spring steel beam properties

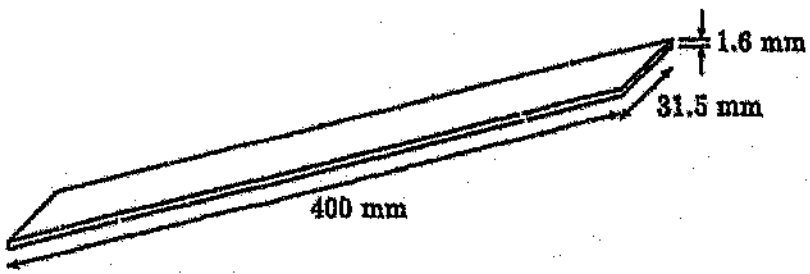

Figure 5.1: Spring steel beam and dimensions

The other components of the test apparatus included the signal conditioning devices, the sensors, actuator and the controller.

5.1.1 Hardware considerations

A number of publications discuss optimal sensor and actuator placement [5, 4, 8]. However, all seem to have an equal number of sensors and actuators, often up to five sensors and actuators on a flexible beam. Besides the difficulties of the limited space along a test rig, the effect of the sensors and actuators is to alter the dynamics of the system considerably, unless sensors such as optical sensors and actuators such as electrodynamic force actuators are employed. The term most papers use to describe the placement of the sensors and actuators is the collocation of sensors and actuators, simply meaning the same physical location of sensor and actuator, so control methods need to be employed to achieve the required results.

Baruh and Choe [5] discuss the issues associated with sensor placement in structural control. Results are presented showing the optimal placement of five sensors for pinned-pinned beam and a tapered bar. Failure of the structure is also considered and backup positions are presented for this purpose. Although the papers by Goh and Lee [25] and Goh and Caughey [24] do not deal exclusively with sensor placement, the stable control methods that are discussed in these papers rely on the fact that the sensors and actuators are collocated.

A further consideration for many researchers in the field of structural control is the selection of sensors and actuators. The selection of an actuator has become the subject of many papers [1, 6, 8, 16], with the vast majority opting for the choice of a piezoelectric crystal used as an actuator. With the success of the piezoelectric crystal due to its properties, a number of papers have been published on the use of piezoelectric film. The use of the film instead of the crystal is due to the fact that the piezoelectric film is a distributed parameter, potentially making the control of a continuous system easier.

The papers discussing the MIMSC technique cite the use of the piezoelectric crystal in the experimental portions of their work. The author together with Wood [26] used a piezoelectric crystal in undergraduate research on active vibration control in flexible structures, and found it to be suitable for the task. A paper relating to this research was published [27], describing the theoretical background and practical implementation of a control system for a flexible structure. The direct velocity feedback system was employed and together with either an electrodynamic shaker or a piezoelectric crystal as the actuator a stable control system was developed.

Bailey and Hubbard [1] and Burke and Hubbard [16] are among the researchers that have published work on active vibration control using a piezoelectric-polymer as the actuator. These works employ a complex mathematical method, whereby the control laws are obtained so that the law can use the distributed parameter actuator. Sadek et al [47] were among other researchers that also discussed the use of distributed parameter actuators, and showed their applicability. Both papers dealt with flexible beams as their test systems.

The use of shape memory alloys as actuators in active vibration control has also been documented. Baz, Imam and McCoy [6] document the feasibility of using shape memory actuators (SMA) in controlling flexural vibrations of a flexible cantilevered beam.

5.1.2 Sensors

The transducers used to detect the vibration of the beam were accelerometers. Accelerometers were chosen primarily due to the fact that a velocity or position of the beam could be estimated from the acceleration signal by an integrator. This was a better route than using for example proximity probes or linear varying displacement transducers (LVDT) since these devices would demand numerical differentiation by the controller, which tends to produce a large amount of noise on the output.

The other reasons for the use of the accelerometers was that Strut Cell accelerometers were avaliable in the laboratory and these are light weight compared with the weight of the beam. Therefore, the dynamics of the beam are not greatly affected by the attachment of the accelerometers on the beam. This can be seen from the theoretical development of the beam equations and transfer function given in section 2.1.3.

All the accelerometers were calibrated against a rotational accelerometer with vendor supplied calibration data before they were used.

The other sensor used was a force transducer. The force transducer was affixed between the actuator and the beam. This was done so that a transfer function between the accelerometers on the beam and the force applied to the beam could be determined. This was described in section 2.2. The calibration constant of the force transducer was taken into account. Although the force transducer was not necessary in the experimental work, other than to monitor the force applied to the beam, the transducer was left in place so as not to affect the beam dynamics that were experimentally determined.

5.1.3 Actuators

A number of actuators had been tested in previous work relating to the subject of vibratic control [26]. These included piezoelectric crystals and electrodynamic shakers.

From preliminary investigations in undergraduate research, the piezoelectric crystal showed promise in the actuation of the control of structural vibration; this has been confirmed by a number of papers [1, 8, 18, 26] which have discussed the use of both piezoelectric polymers and crystals as the actuating component. The main drawbacks in the use of piezoelectric materials is the large amount of energy that is required for the best performance of the crystal and the cost of either the crystal or the polymer. The crystal used previously was approximately 5cm in length, which required up to a maximum of about 2500 volts in order to extract the true value from the actuator.

The electrodynamic shaker proved to be an excellent actuator. Although, the shaker that was avaliable was too large for the cantilevered beam, previous work showed that the electrodynamic shaker would counteract the vibration in the beam quite easily. However, the design that was employed was probably an over design. This particular electrodynamic shaker would also not always be avaliable, and the cost of new smaller shakers was too much. Therefore, an alternative actuation system was sought.

The actuator that was decided on was based on the same principal as the electrodynamic shaker system, but had a much smaller peak force output, and could be

permanently fixed to the test structure. This actuator was a load speaker coil and provided a cost effective solution to the problem of actuation.

5.1.4 Signal conditioners

The main signal conditioner used was that of an amplifier for the actuator. This provided a current large enough to drive the speaker coil from the controller output voltage. The amplifier is fitted with a current feedback module, so that the voltage input to the actuator is proportional to the force applied to the beam by the actuator. This was measured by taking a transfer function between the voltage input to the actuator and the force applied to the beam, and it was found that the voltage was indeed proportional to the force.

The use of analogue filters were not necessary, since it was decided that the filtering would be done digitally, providing for greater flexibility. However, analogue filters would be used to compare with those that had been numerically designed and digitally implemented.

5.1.5 Controller

Up until very recently experimental work that has been carried out employed the use of analogue controllers. Few papers such as [15] and [11] discuss the use of digital controllers. The first paper makes reference to a specific digital signal processor, named the TMS320C20 DSP processor. This type of hardware is of particular interest in the current research, as the project will use a digital processor of the same type except for the added advantage of using floating point processing. The other paper discusses the AT&T DSP32C processor for use as the digital controller. The use of this processor as a controller is shown to be employed so as to successfully implement a very complex mathematical algorithm, such as the Wiener–Hopf optimisation routine as described by [11].

Hanselmann [28], discusses the processors on the market until 1987, that could be employed as digital controllers. Furthermore, the pitfalls as well as advantages in the use of digital techniques are outlined. This paper gives a good overview of the current digital processors commercially available and allows an easy selection of the best processor for the particular application. Hanselmann also compares some of the better known processors, by implementing a control algorithm. Although the digital filters that are used as examples to demonstrate the capabilities of the DSP (digital signal processors) are fairly simple systems, the comparison of floating and fixed point processors is evident.

In previous work an analogue computer was used as the controller. Although, this allowed for the time delay between samples in a digital controller to be ignored, the restrictions of the analogue system were noted. The main restrictions were the number of integrators and summers present. In addition to this it was found that the integrators saturated very quickly, requiring a reset for continued operation.

It was decided that a solution to these problems would be the use of a digital controller, with the flexibility of the controller being the main advantage. This also allowed for a more complex system, if the digital controller catered for high speed computation. The use of a digital signal processor based controller was ideal for

this application. The controller used in the experimental implementation is the TMS320C30 floating point digital signal processor (DSP) card.

5.2 Digital filtering

As discussed in the previous section, digital filtering was used in place of analogue filters. The number of filters required, made it necessary to find an alternative method to the use of analogue filters to make it economically viable.

A number of filters were necessary. The first being the filter that would attempt to eliminate the higher frequency signals; those above the range of the modes that were to be controlled. The other filters were the filters necessary to isolate a specific mode of vibration. This was needed since the MIMSC method ranks the modes in order of their modal energy and to do this the amplitude of each mode is individually required.

5.2.1 Specific filters

The required filters were designed using MATLAB and were based on the Chebyshev filter design. By using the Chebyshev filters a steeper roll-off with a lower order filter could be found, while still maintaining a flat (monotonic) passband. This is achieved by allowing for equiripple in the stopband, which is kept to a minimum. This is shown diagrammatically in Figure 5.2, which has an exaggerated ripple in the stopband to make Figure 5.2 more meaningful.

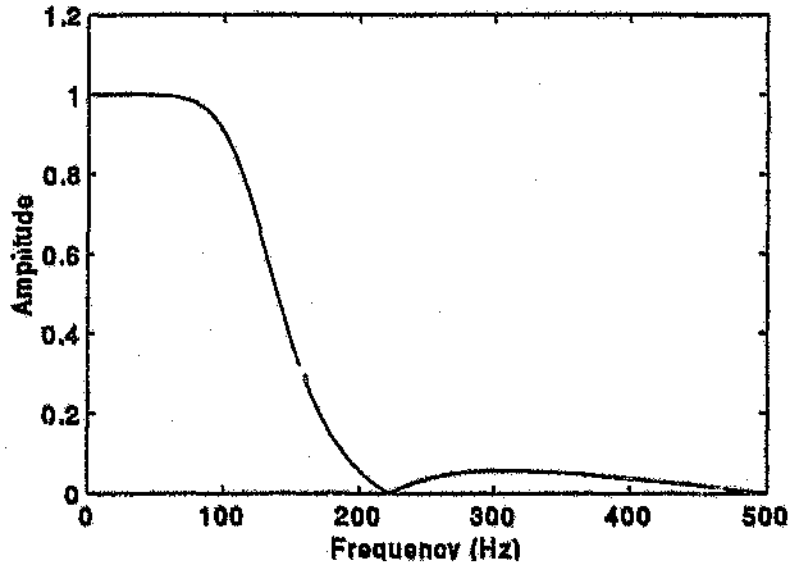

Figure 5.2: A typical Chebyshev type-II filter.

The design is done using the bilinear transformation technique. This technique requires the presence of an existing low pass analogue filter. The differential equation is integrated, but a numerical approximation to the integral is used and is based on

the trapezoidal rule. The bilinear transformation is applied, which maps the s–plane onto the z–plane by the mapping [44]

$$s = \frac{2}{T}\frac{1-z^{-1}}{1+z^{-1}} \qquad (5.1)$$

where T is the sampling period.

It was found that when the filters were designed, if the numerator of the filter had a very small term (typically 1×10^{-14}) these filters would not behave properly when implemented on the controller. Therefore, is was necessary to design the filters in such a manner that as gradual a roll–off at could be catered for would be incorporated. Figures 5.3 to 5.6 show the numerical frequency response of the filters designed to filter out frequency elements not pertaining to that particular mode of vibration. Figures 5.4 and 5.5 are both designed around mode 2, since it was found that by applying a low–pass and then a high–pass filter, a wider pass band range could be found rather than using a band–pass filter.

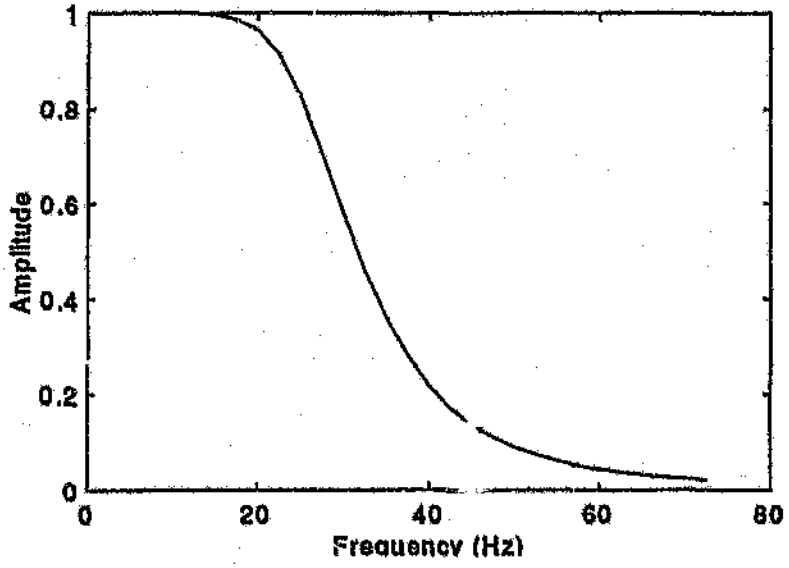

Figure 5.3: Low–pass filter containing only mode 1 frequency elements.

5.2.2 Integration

It was also decided to use a filter as an integrator. This was because the software that communicates with the card has built in libraries that could implement digital filters. The integrator is based on the trapezoidal rule and because of the high sampling frequency a more complex approximation for example Simpson's rule was not necessary.

The trapezoidal rule is based on the approximation of the area under a curve and between samples as being a trapezoid. The approximation of this area is clearly shown in Figure 5.7.

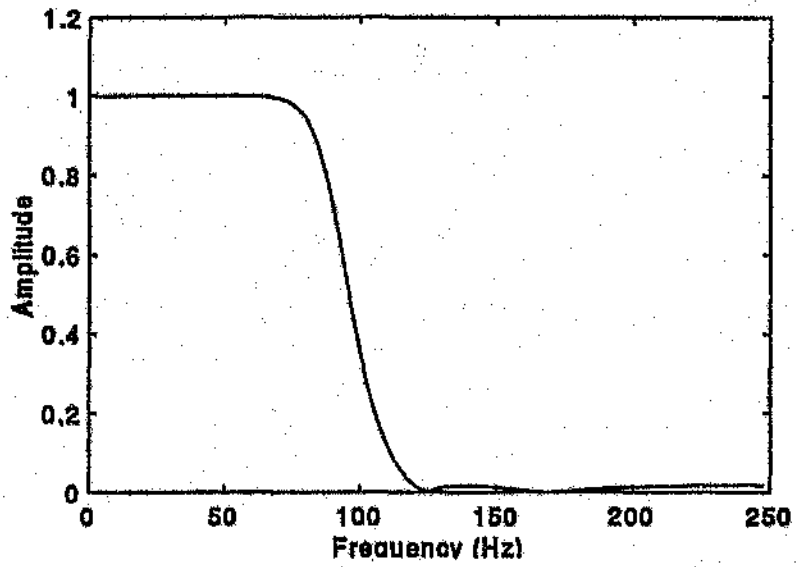

Figure 5.4: Low-pass filter containing mode 1 and 2 frequency elements.

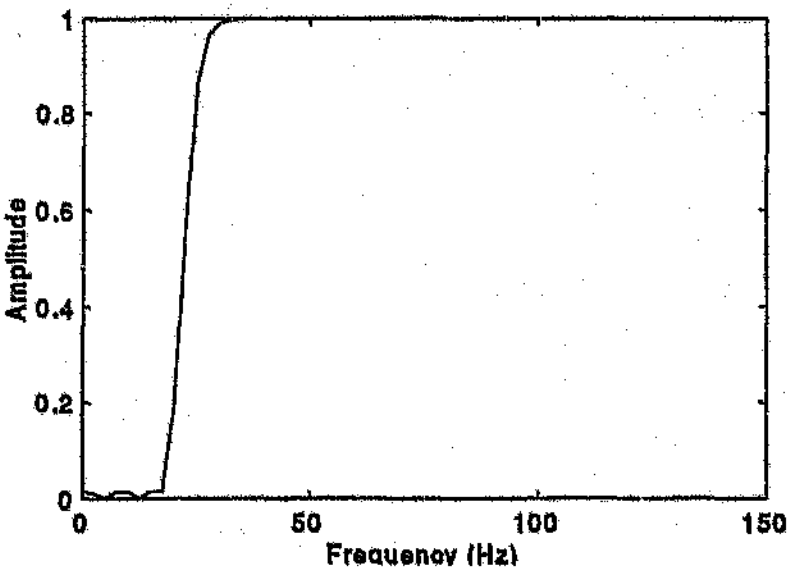

Figure 5.5: High-pass filter containing mode 2 and higher frequency elements.

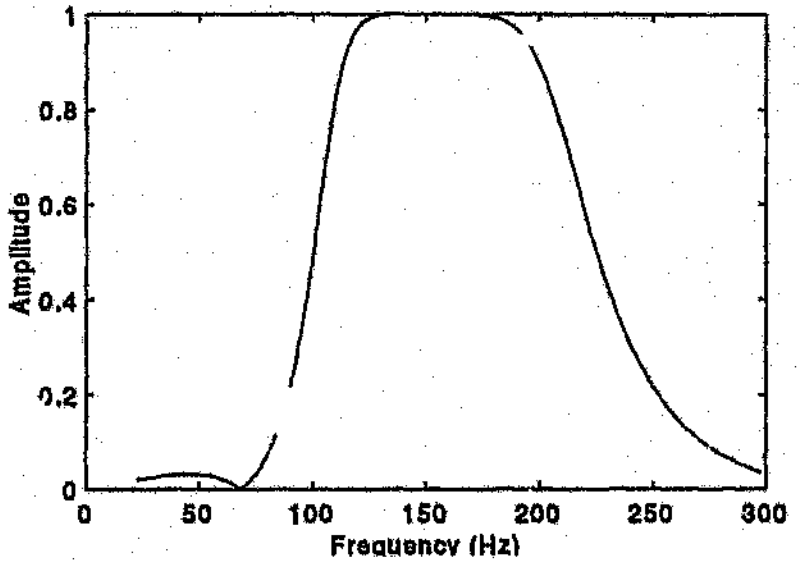

Figure 5.6: Band-pass filter containing only mode 3 frequency elements.

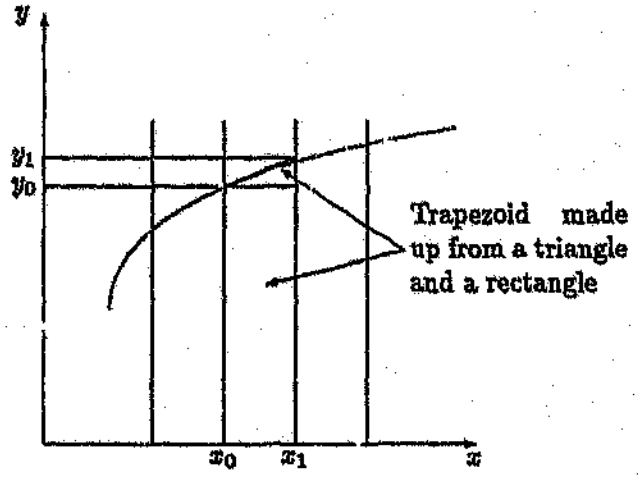

Figure 5.7: The trapezoid between samples.

Since we know that the bilinear transformation is based on the trapezoidal rule, and from Laplace transformation tables an integral is given as $1/s$, we can use these two equations together to design a filter that will be an integrator. The bilinear transformation is given as

$$s = \frac{2}{T}\frac{1-z^{-1}}{1+z^{-1}} \tag{5.2}$$

Now using the fact that an integral is $1/s$ and combining with equation 5.2, the integrator becomes

$$\frac{1}{s} = \frac{T/2+T/2z^{-1}}{1-z^{-1}} \tag{5.3}$$

The frequency response of the filter is shown in Figure 5.8. It can be seen that as the

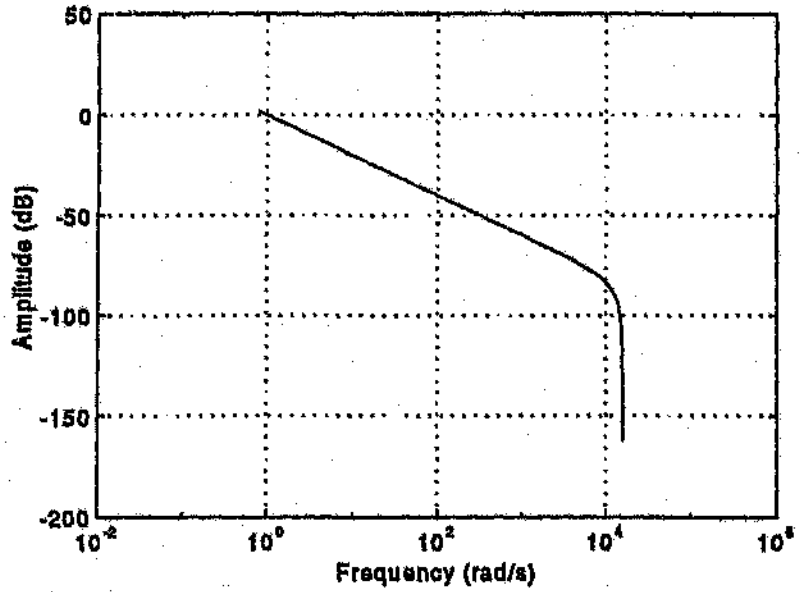

Figure 5.8: Frequency response of the integrator.

filter approaches the Nyquist frequency (half the sampling frequency) the frequency response deviates from a true integrator. Due to the high frequency content at which the filter deviates from an integrator, this should not have an effect on the system being controlled.

5.3 Input disturbance

As discussed (Chapter 4), it was decided to use an impulse force as a disturbance input to the cantilevered beam. The impulse hammer was used for this purpose and although the disturbance force was over a finite time period it could be closely compared with the numerical impulse force. Figure 5.9 shows a typical response, in the time domain, of an impulse force due to the action of an impulse hammer.

The force exerted by the hammer on the beam (for each test) was measured so that all the results could be scaled and so compared with the numerical solutions and with each other.

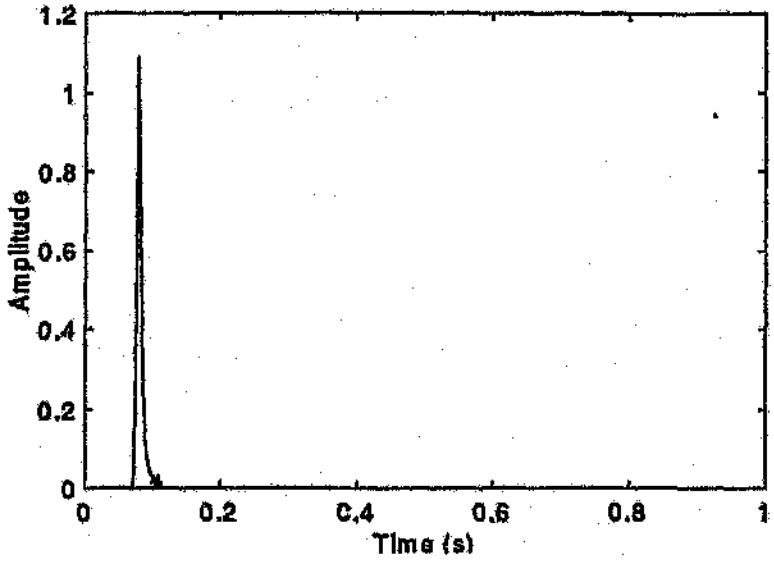

Figure 5.9: Force versus Time for a typical measured impulse force.

5.4 Implementation

With the basic building blocks for the physical implementation of a control law in place, the programs could be written to control the vibration of the beam. This was not an easy task, since the software that is used to communicate with the TMS320C30 card is not user friendly. Furthermore, the budget did not allow for better software to make the implementation of the control systems simpler. However, results for each control method discussed in Chapters 3 and 4 were found and are presented here.

5.4.1 Uncontrolled response

To compare the controlled response in each case, the experimental uncontrolled response of the cantilevered beam is shown here. The beam is excited by an impulse from an impulse hammer and the response is measured by means of two accelerometers. The results presented show physical displacement from each of the two positions. This is consistent with the numerical results shown.

Figures 5.10 and 5.11 show the uncontrolled, free vibration of the cantilevered beam.

These results compare well with the predicted ones shown in Chapter 4. Hence, the parameter estimation techniques used to develop a model describing the cantilever beam are satisfactory and therefore may be used to predict the physical response of a similar beam without the need for experimental testing.

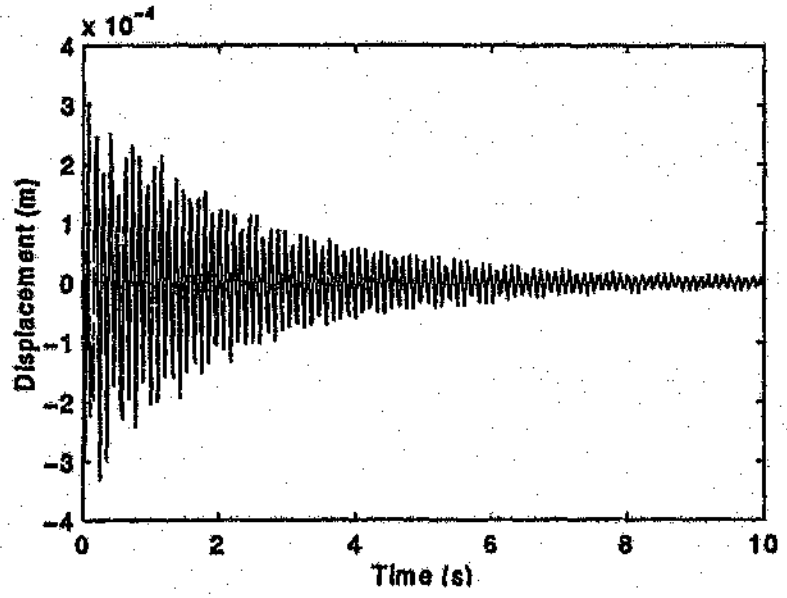

Figure 5.10: Uncontrolled response at position 1.

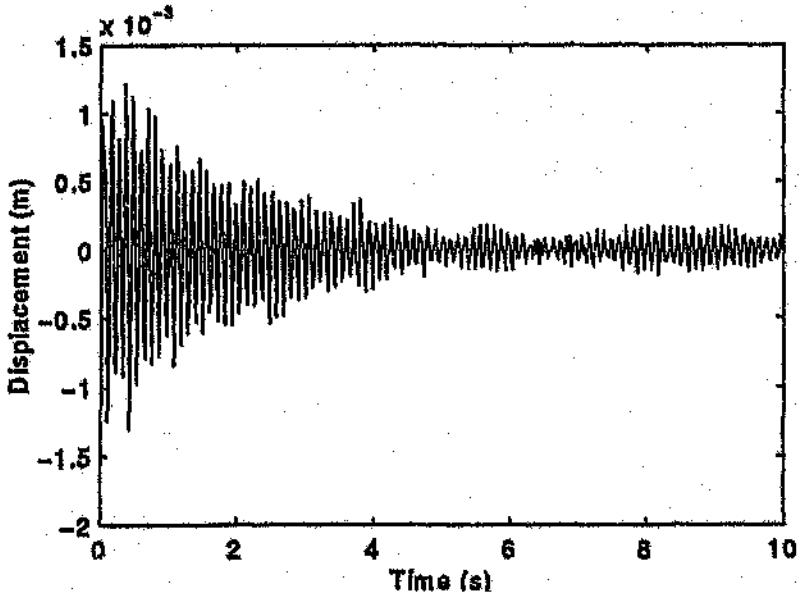

Figure 5.11: Uncontrolled response at position 2.

5.4.2 Direct velocity feedback

From Chapters 3 and 4, the background to the velocity feedback system is given and the applicable block diagram is shown in Figure 5.12.

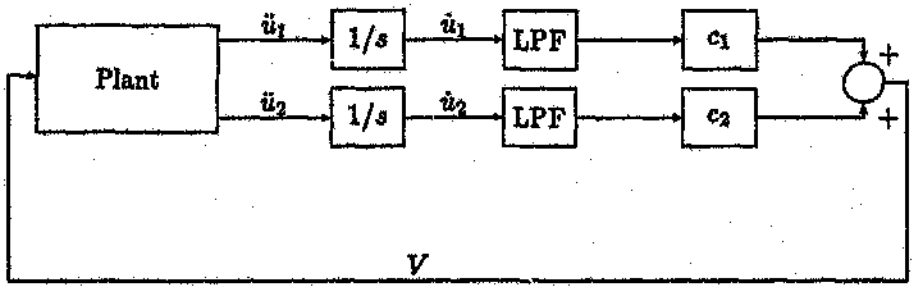

LPF = low pass filter

Figure 5.12: Block diagram of the direct velocity feedback system.

Figure 5.12 shows the plant as a "black box" type setup. This is consistent with the experimental setup since the plant is the beam being controlled and exists as a single entity. This is clearly shown in Figure 5.13.

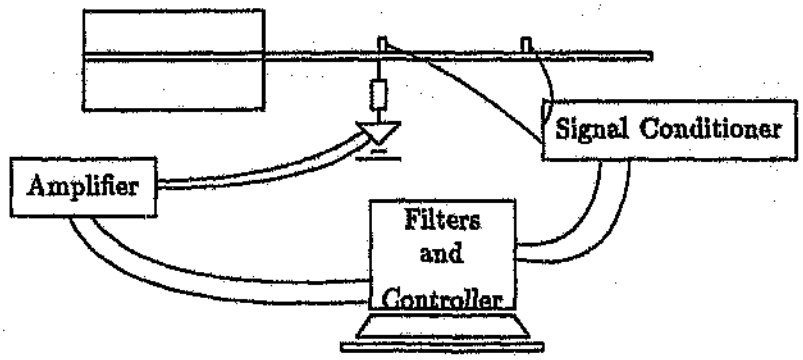

Figure 5.13: Experimental setup for the direct velocity feedback system.

As discussed the relevant digital filters were designed using MATLAB. Different filters were used to compare results and show the necessity of eliminating the higher frequency content for the accelerometers. Furthermore, analogue filters were also used to check the efficiency of the equivalent digital filters.

Three sets of results are presented for the direct velocity feedback method. The first results shown are for the control of the first two modes, with the filtering being carried out by the analogue filters. These results are shown in Figures 5.14 and 5.15. Figures 5.16 and 5.17 show the controlled forced response of the beam, using the digital filters and the last results presented for the direct velocity feedback method, show the importance of filtering out the higher order modes. The response shown in Figures 5.18 and 5.19 are results of controlled beam displacement neglecting to eliminate the energy from the higher order modes. Therefore, spillover to those higher order modes results and the response to an impulse force input shows a neutrally stable beam.

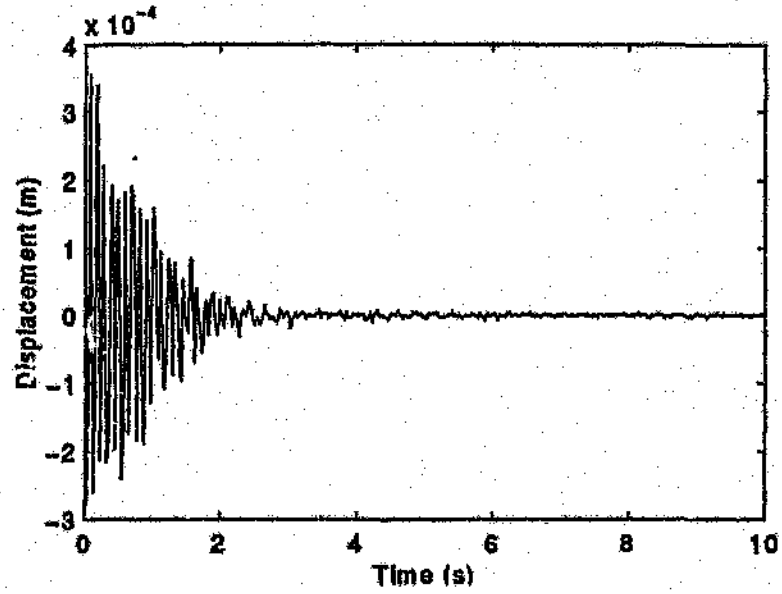

Figure 5.14: Controlled forced response using analogue filters, at position 1.

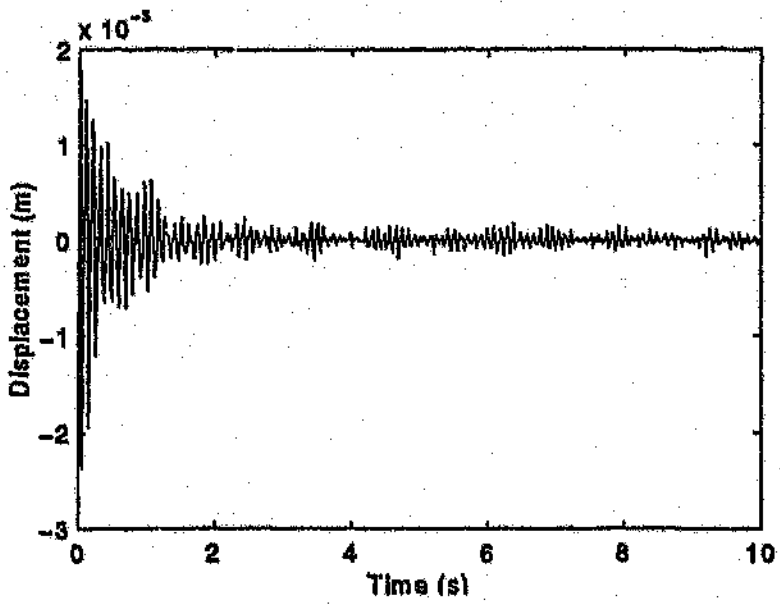

Figure 5.15: Controlled forced response using analogue filters, at position 2.

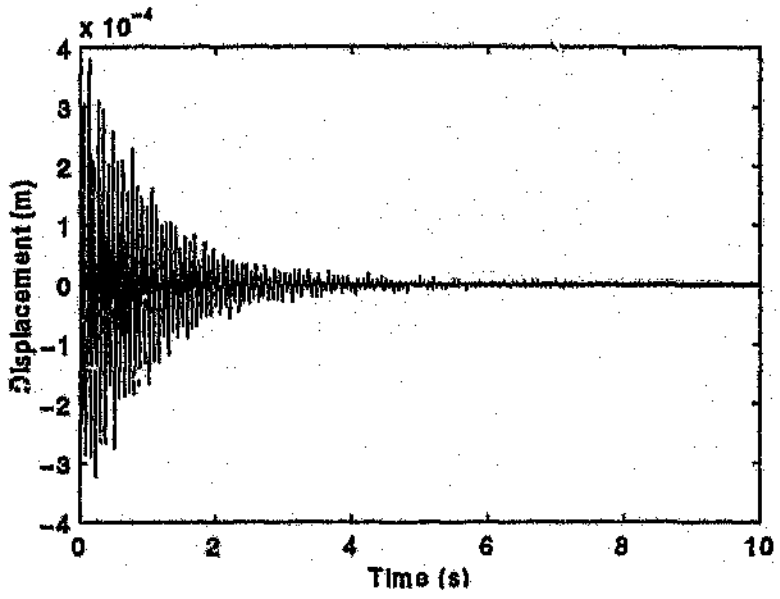

Figure 5.16: Controlled forced response using digital filters, at position 1.

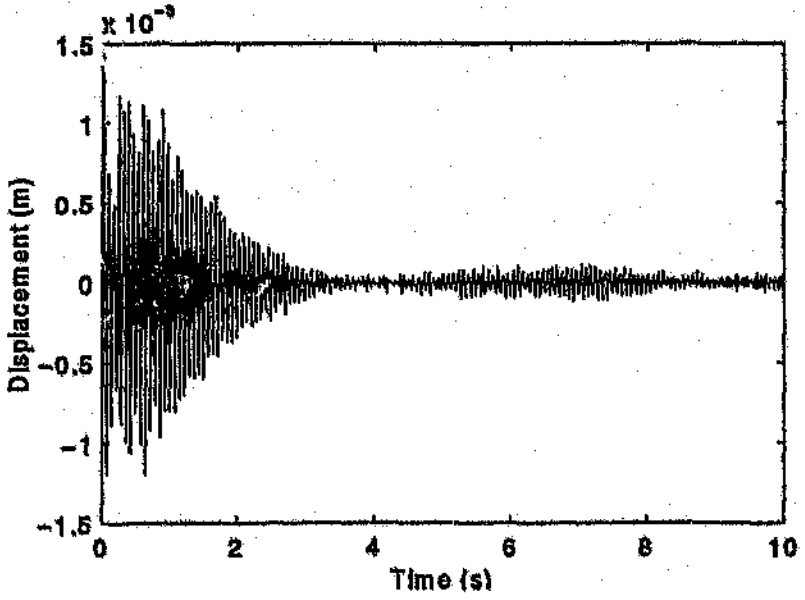

Figure 5.17: Controlled forced response using digital filters, at position 2.

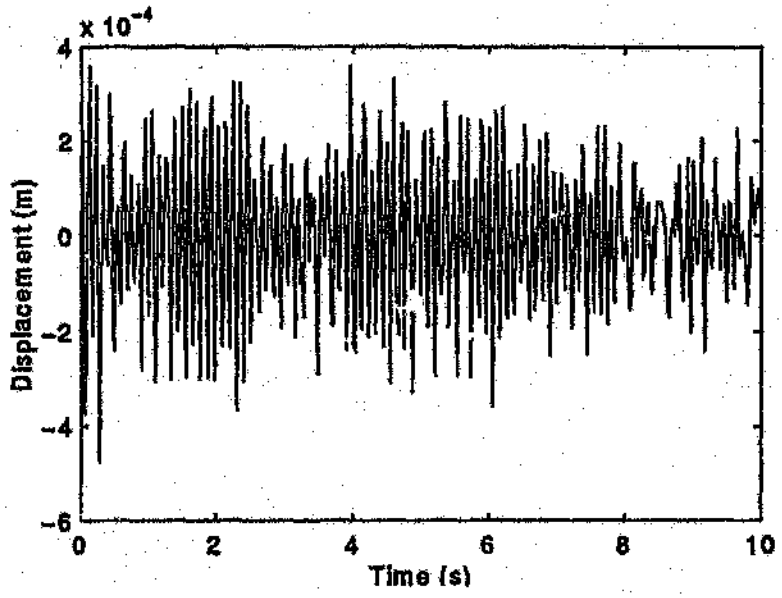

Figure 5.18: Controlled forced response without filters, at position 1.

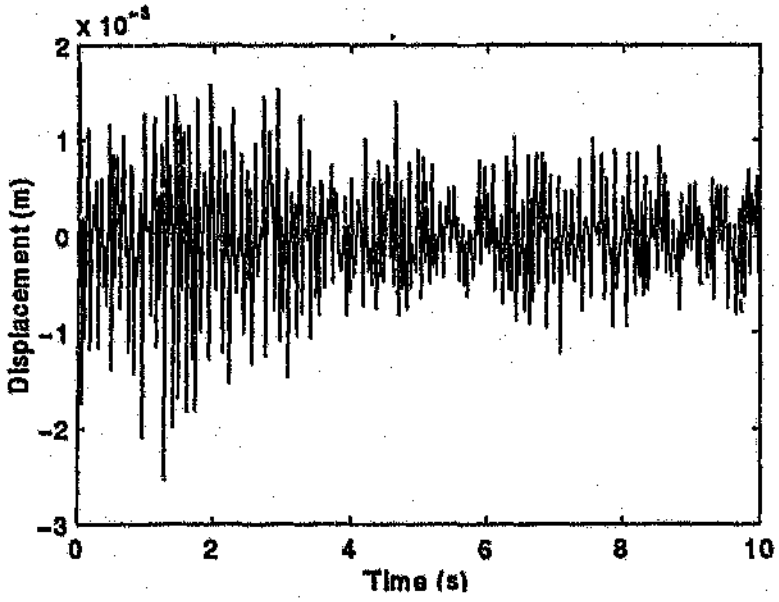

Figure 5.19: Controlled forced response without filters, at position 2.

5.4.3 The MIMSC method

The experimental apparatus is exactly the same as that given in the previous section. The con ol philosophy, however, is different and only one accelerometer is used. The other accelerometer is left in place so that the dynamics of the beam are not affected.

The block digram of the MIMSC control technique experimental apparatus is shown in Figure 5.20.

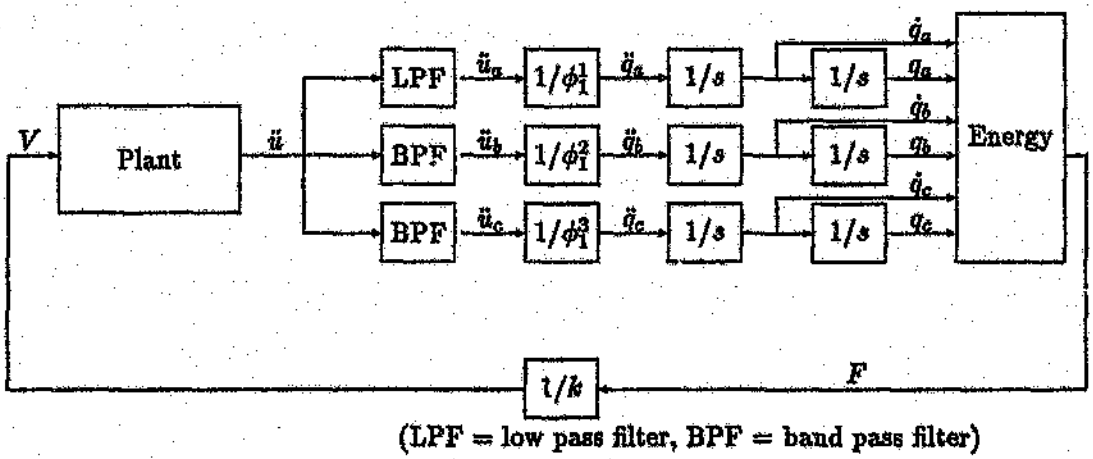

(LPF = low pass filter, BPF = band pass filter)

Figure 5.20: Block diagram for the MIMSC control theory.

The results of the MIMSC test with an impulse force input is shown in Figure 5.21.

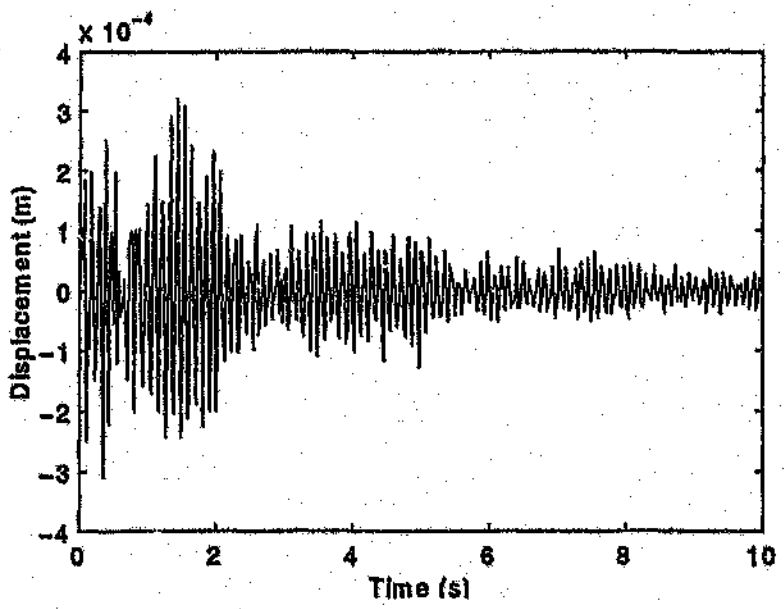

Figure 5.21: Controlled forced response using the MIMSC technique.

Figure 5.21 does not show usable results. It was difficult to disturb the beam with a much smaller excitation and therefore form a basis of comparison with the numerical results. However, Figure 5.21 is consistent with the numerical solution in that the MIMSC technique will not show an improvement on the free response without a larger control force. This was not possible with the speaker coil used in these tests.

5.5 Discussion

The physically measured results compare well with those generated by numerical calculation.

For the direct velocity feedback method, is it evident that the analogue filters are more efficient than their equivalent digital filters. However, the cost of the analogue filters make the use of digital filters very appealing. Furthermore, the variation in the two sets of results is not that large such that the digital filter solution should be ignored. The necessity of the filters as discussed in Chapters 3 and 4 is clearly demonstrated in Figures 5.18 and 5.19. As shown, the beam does not necessarily become totally unstable without the higher order modes being filtered out; a neutrally stable response may be the result. Either solution is unwanted and therefore spillover into the higher order modes must be accounted for.

The experimental results for the direct velocity feedback method (Figures 5.14 and 5.15) appear much better than the numerical results (Figures 4.9 and 4.10). This is due to the fact that the a voltage just larger than the assumed 10 volts could be supplied to the actuator.

Only two analogue filters were available and therefore only digital filters were used in the MIMSC tests. As with the numerical results, the measured results for the MIMSC method show that the tests consistent with the direct velocity feedback tests display a worse response than the free vibration results. It was not possible to excite the beam with a smaller magnitude force and a different actuator was not avaliable, so the results reflected in the analytical work are not repeated here.

Chapter 6

Conclusions and Recommendations

6.1 Conclusions

6.1.1 General

A test structure consistent with previous work [7, 18, 26, 47, 49] was used and proved to be an ideal rig for testing of structural vibration. As the theoretical work shows, a steel beam can easily be extended to compare with large flexible structures.

The mathematical model developed from experimental modal parameters proved better than a pure analytical approach. The model was shown to compare well with experimental results for both the free and forced vibration cases. Furthermore, the model behaved as expected with the addition of a control law. This is seen by comparing the results in Chapters 4 and 5. With the well behaved response of the model, it is evident that a steel beam is a good test structure to use in structural vibration research. It is well defined in the theory, and even a purely analytical approach to the mathematical model will yield results comparable with the experimental ones.

6.1.2 Control Techniques

The selection of the control laws was based on a literature review. Two techniques were selected, namely the direct velocity feedback and the Modified Independent Modal Space Control (MIMSC) methods.

The direct velocity feedback method was a good starting point. The experimental behaviour of the steel beam was consistent with the analytical results. Furthermore, because of the reduced complexity of this technique it is less demanding on hardware and therefore cost. The direct velocity feedback method is a useful structural vibration control tool.

The results of the MIMSC method showed that although this technique had promise, it demanded a large amount of energy to be applied to the beam. The experimental results were not conclusive and further work needs to be done to allow for a larger control force.

Although the basic control principle of the two techniques is similar, the control philosophy is different. The direct velocity feedback method uses as many sensors as modes to be controlled, whilst the MIMSC method has a "time sharing" mechanism which uses a reduced number of sensors compared with modes to be controlled. Therefore, each technique would be used for the solution to different structural vibration control problems dependent on the problem constraints.

6.1.3 Digital control

The digital signal processing (DSP) card was ideal for the application of digital control. The software, however, used in conjunction with the TMS320C30 chip was not user friendly and could be improved upon. The budget did not allow for improved software and therefore the programming of the controllers took more time than expected.

The high speed of the DSP card did allow for the complexity of the MIMSC method as well as the digital filters to be accurately implemented. Therefore, the advantage of the digital type controller over the analogue methods is significant and digital control methods should be pursued.

6.2 Recommendations for further work

A number of areas of the research are well defined and further work in these areas is not necessary; they are:

- The selection of a test rig. The cantilevered beam has a well behaved frequency response to an input disturbance and it is analytically well defined.
- The use of the direct velocity feedback method, other than an extension to more controlled modes.
- The selection of a digital controller. The TMS320C30 based DSP card is ideal for digital control. This is due to its high speed and floating point processing capabilities. However, currently not enough input and output channels are available.

From this list it is clear that further work on the MIMSC and other control laws (particularly [53]) is the path to follow to continue with this research. Once better software and more channels are available for the DSP card, higher modes and more complex systems may be analysed.

The test rig could be improved upon. The selection of different sizes and materials for the cantilevered beam would lower the frequency at which the modes present themselves, making it easier to control more modes of vibration.

Different actuators could be tested. As discussed, both the piezoelectric crystal and the electrodynamic shaker show promise as actuators in structural vibration control and these should be explored further.

The direct velocity feedback method is well documented and the results presented in this dissertation are consistent with those results. Further work is not necessary

to verify the applicability of this control technique. The advantage gained over controlling more modes, however, may be of interest.

The MIMSC technique needs further work. Specific attention should be paid to the need of a larger control force for the MIMSC method, and therefore a speaker coil as an actuator may not be the best solution. The MIMSC method should also show a far improved frequency response by extending the experimental work to the use of more than one actuator.

It is demonstrated in this research that state space control theory does not address the spillover problem. Therefore, other control techniques such as QFT [53] should be analysed with attention to the need to filter out the "spillover" onto the modes that are not being controlled.

Bibliography

[1] Bailey T & Hubbard JE, "Distributed Piezoelectric–Polymer Active Vibration Control of a Cantilever Beam," Journal of Guidance and Control, Vol 8 No. 5, 1985, pp 605–611.

[2] Balas MJ, "Trends in Large Space Structural Control Theory: Fondest Hopes, Wildest Dreams," IEEE Transactions on Automatic Control, Vol AC-27 No. 3, June 1982, pp 522–535.

[3] Balas MJ, "Feedback control of flexible systems," IEEE Transactions on Automatic Control, Vol AC-23, 1982, pp 673–679.

[4] Balas MJ, "Direct Velocity Feedback Control of Large Space Structures," Journal of Guidance & Control, Vol 2, 1978, pp 252–253.

[5] Baruh H & Choe K, "Sensor Placement in Structural Control," Journal of Guidance and Control, Vol 13 No. 3, 1990, pp 524–533.

[6] Baz A, Imam K & McCoy J, "Active vibration control of Flexible Beams using Shape Memory Actuators," Journal of Sound and Vibration, Vol 140, 1990, 437–456.

[7] Baz A & Poh S, "Experimental implementation of the Modified Independent Modal Space Control method," Journal of Sound & Vibration, Vol 139, 1990, pp 133–149.

[8] Baz A & Poh S, "Performance of an Active control system with Piezoelectric actuators," Journal of Sound & Vibration, Vol 126, 1988, pp 331–341.

[9] Baz A, Poh S & Studer P, "Modified independent modal space control method for active control of flexible systems," Proceedings of the IMechE Part C: Journal of Mechanical Engineering Science, 1989, pp 103–112.

[10] Belvin WK & Park KC, "Structural Tailoring and Feedback Control Synthesis: An Interdisciplinary Approach," Journal of Guidance and Control, Vol 13 No. 3, 1990, pp 424–429.

[11] Bennet WH, "Digital signal processing methods for control of vibrations in structures," Proceedings of the Conference on Recent advances in active control of sound and vibration, April 1991, pp 783–793.

[12] Bleiloch PA & Mingori DL, "Robust Linear Quadratic Gaussian Control for Flexible Structures," Journal of Guidance & Control, Vol 13 No. 1, 1990, pp 66–72.

[13] Bontsema J & Curtain RF, "A Note on Spillover and Robustness for Flexible Systems," IEEE Transactions on Automatic Control, Vol 33 No. 6, June 1988, pp 567–569.

[14] Borghesani C, Chiat Y & Yaniv O, "MATLAB QFT Toolbox," The Mathworks, 1995.

[15] Burdisso RA & Fuller CR, "Theory of feedforward controlled system Eigenproperties," Journal of Sound & Vibration, Vol 153, 1992, pp 437–451.

[16] Burke SE & Hubbard JE, "Distributed Actuator Control Design for Flexible Beams," Automatica, Vol 24, 1988, pp 619–627.

[17] CADA–PC Reference Manual, LMS, 1990.

[18] Chen CI, Napolitano MR & Mucino V, "Applications of the MIMSC method for active control of vibrations of a Cantilever Beam: A Numerical Study," Proceedings of the Conference on Recent advances in active control of sound and vibration, April 1991, pp 631–654.

[19] Czajkowski EA, Preumont A & Haftka RT, "Spillover Stabilization of Large Space Structures," Journal of Guidance & Control, Vol 13 No. 6, 1990, pp 1000–1007.

[20] Ellis RW & Mote CD, "A Feedback Vibration Controller for Circular Saws," Journal of Dynamic Systems, Measurement, and Control, Vol 101, March 1979, pp 44–49.

[21] Ewins DJ, "Modal Testing: Theory and Practice," Research Studies Press Ltd., 1986, pp 19–59 & 153–170.

[22] Fukuda T, Arai F, Hosogai H & Yajima N, "Modelling and Control of Torsional Vibrations in a Flexible Structure," JSME International Journal, Vol 30 No. 264, 1987, pp 976–981.

[23] GenRad Reference Manual, GenRad, 1982.

[24] Goh CJ & Caughey TK, "On the stability problem caused by finite actuator dynamics in the collocated control of large space structures," International Journal of Control, Vol 41 No. 3, 1985, pp 787–802.

[25] Goh CJ & Lee TH, "Adaptive modal parameters identification for collocated position feedback vibration control," International Journal of Control, Vol 53 No. 3, 1991, pp 597–617.

[26] Grobbelaar BJ & Wood GD, "Active Vibration Control of a Cantilevered Beam," BSc Final Year Design Project, School of Mechanical Engineering, University of the Witwatersrand, 1991.

[27] Grobbelaar BJ, Wood GD & Constançon CP, "Application of Modal Control to Flexible Structures," R&D Journal, Vol 8 No. 2, July 1992, pp 18–24.

[28] Hanselmann H, "Implementation of Digital Controllers – A Survey," Automatica, Vol 23 No. 1, 1987, pp 7–32.

[29] Horowitz H, "Quantitative feedb: k theory," IEE Proceeding Part D, Vol 129 No. 6, Nov 1982, pp 215–226.

[30] Horowitz H, "Survey of quantitative feedback theory (QFT)," Internatinal Journal of Control, Vol 53 No. 2, 1991, pp 255–291.

[31] Horowitz H, "Quantitative Feedback Design Theory ," QFT Publications, Vol 1, 1992. IEE Proceeding Part D, Vol 129 No. 6, Nov 1982, pp 215–226.

[32] Hughes P, "Passive dissipation of energy in large space structures," Journal of Guidance and Control, Vol 3, 1980, pp 380–382.

[33] Hughes P & Skelton R, "Controllability and observability for flexible spacecraft," Journal of Guidance and Control, Vol 3, 1980 pp 452–459.

[34] Joshi SM, "Optimal member damping controller design for LSS," Journal of Guidance and Control, Vol 3, 1980, pp 378–380.

[35] Joshi SP, Vincent TL & Lin YC, "Control for Energy Dissipation in Structures," Journal of Guidance and Control, Vol 13 No. 4, 1990, pp 751–753.

[36] Livneh R & Slater GL, "Adaptive controller for wing flutter with unmeasurable excitations and unmodelled dynamics," International Journal of Control, Vol 53 No. 2, 1991, 293–309.

[37] Maciejowski JM, "Multivariable Feedback Design," Addison–Wesley Publishing, 1989, pp 222–262.

[38] MATLAB 4.0 Reference Manual, The Mathworks Inc, 1992.

[39] Meirovitch L, "Analytical methods in Vibrations," MacMillian Co., 1967, pp 135–148.

[40] Meirovitch L & Baruh H, "Control of Self–Adjoint Distributed–Parameter Systems," Journal of Guidance and Control, Vol 5, 1982, pp 59–66.

[41] Meirovitch L & Baruh H, "Robustness of the Independent Modal Space Control Method," Journal of Guidance and Control, Vol 6, 1983, pp 20–25.

[42] Meirovitch L, Baruh H & Öz H, "A comparison of control techniques for large flexible systems," Journal of Guidance & Control, Vol 6, 1983, pp 302–310.

[43] Morgül Ö, "Dynamic Boundary Control of an Euler–Bernoulli Beam," IEEE Transactions on Automatic Control, Vol 37 No. 5, May 1992, pp 639–642.

[44] Oppenheim A.V. & Schafer R.W., "Digital Signal Processing," Prentice–Hall International, 1975, pp 195–226.

[45] Öz H, Farag K & Venkayya VB, "Efficiency of Structure–Control Systems," Journal of Guidance and Control, Vol 13 No. 3, 1990, pp 545–554.

[46] Palm WJ, "Control Systems Engineering," John Wiley & Sons, 1986, pp 311–350 & 523–628.

[47] Sadek IS, Adali S, Sloss JM & Bruch JC, "Optimal Distributed Control of a Continuous Beam with damping," Journal of Sound & Vibration, Vol 117, 1987, pp 207–218.

[48] Schaechter DB, "Hardware Demonstration of Flexible Beam Control," Journal of Guidance & Control, Vol 5, 1982, pp 48–54.

[49] Schäfer BE & Holzach H, "Experimental research on Flexible Beam Modal Control," Journal of Guidance and Control, Vol 8, 1985, pp 597–604.

[50] SIMULINK 1.2c Reference Manual, The Mathworks Inc, 1992.

[51] Tse FS, Morse IE & Hinkle RT, "Mechanical Vibrations," Allyn and Bacon Inc., 1989, pp 253–288.

[52] Williams T & Juang J, "Pole/Zero Cancellations in Flexible Space Structures," Journal of Guidance and Control, Vol 13 No. 4, 1990, pp 684–690.

[53] Yaniv O & Horowitz I, "Quantitative feedback theory for active vibration control synthesis," International Journal of Control, Vol 51 No. 6, 1990, pp 1251–1258.

Author: Grobbelaar Brett James.
Name of thesis: Active vibration control of a structure using digital control.

PUBLISHER:
University of the Witwatersrand, Johannesburg
©2015

LEGALNOTICES:

Copyright Notice: All materials on the University of the Witwatersrand, Johannesburg Library website are protected by South African copyright law and may not be distributed, transmitted, displayed or otherwise published in any format, without the prior written permission of the copyright owner.

Disclaimer and Terms of Use: Provided that you maintain all copyright and other notices contained therein, you may download material (one machine readable copy and one print copy per page)for your personal and/or educational non-commercial use only.

The University of the Witwatersrand, Johannesburg, is not responsible for any errors or omissions and excludes any and all liability for any errors in or omissions from the information on the Library website.